

**Functional analysis of the N-terminal domains of agrin by recombinant
eucaryotic expression**

In a u g u r a l - D i s s e r t a t i o n

zur

Erlangung des Doktorgrades

der Mathematisch-Naturwissenschaftlichen Fakultät

der Universität zu Köln

vorgelegt von

Uwe Winzen

aus Köln

Köln, 2003

Berichterstatter: Prof. Dr. S. Waffenschmidt

Prof. Dr. M. Paulsson

Prof. Dr. R. Sterner

Tag der mündlichen Prüfung:

5. Mai 2003

Dedictated to my family

Table of contents

1. Introduction	1
1.1 Binding to laminin-1	4
1.2 Fusion protein with NGF	9
1.3 Glycosylation of agrin.....	10
1.4 Neurite outgrowth inhibition by agrin	11
1.5 The episomal expression system in human embryonic kidney cells (HEK) and choice of Tag module	12
1.6 Aim of the project	16
2. Methods and Materials	17
2.1 Molecular Biology	17
2.1.1 PCR	17
2.1.2 Site-directed mutagenesis	19
2.1.3 Agarose gel electrophoresis	21
2.1.4 DNA gel elution.....	22
2.1.5 Endonuclease digestion.....	22
2.1.6 DNA quantification.....	22
2.1.7 Dephosphorylation.....	22
2.1.8 Ligation	23
2.1.9 Production of competent bacteria	23
2.1.10 Bacterial “heat shock” -transformation.....	24
2.1.11 DNA-purification.....	24
2.1.12 Sequencing.....	24
2.2 Protein biochemistry	25
2.2.1 SDS gel electrophoresis	25
2.2.2 Western blotting.....	25
2.2.3 Construction, expression and purification of recombinant protein.....	25
2.2.4 Solid phase binding assay	26
2.2.5 N-Glycanase treatment.....	27

Table of contents

2.2.6 Chondroitinase ABC digestion	28
2.2.7 Heparitinase digestion.....	28
2.2.8 Limited tryptic digestion.....	28
2.3 Cell Culture	29
2.3.1 Cells	29
2.3.2 Trypsinization	29
2.3.3 Transfection	29
2.3.4 Selection.....	30
2.3.5 Protein expression.....	30
2.3.6 Neurite outgrowth assays.....	30
2.4 Histology	31
2.4.1 Disruption and regeneration of the retinal basal lamina	31
2.5 Equipment	32
2.6 Solutions, buffers, and media	33
2.7 Antibodies	35
2.7.1 Primary antibodies	35
2.7.2 Secondary antibodies	35
3. Results	36
3.1 Binding to laminin-1	40
3.2 Fusion protein with NGF	47
3.3 Glycosylation of agrin.....	50
3.3.1 Expression of N-terminal agrin fragments.....	50
3.3.2 Localization of the GAG attachment sites in PF9	53
3.3.3 Localization of the GAG attachment sites in PF7.....	56
3.4 Neurite outgrowth inhibition by agrin	58
4. Discussion.....	61
4.1 Binding to laminin-1	61
4.2 Fusion protein with NGF	64
4.3 Glycosylation of agrin.....	65

Table of contents

4.3.1 GAG attachment sites of agrin.....	65
4.3.2 Function of GAGs in agrin	69
4.4 Neurite outgrowth inhibition by agrin	70
5. Literature	72
6. Zusammenfassung	79
7. Abstract.....	81
8. Acknowledgments	83

1. Introduction

Agrin is a large, multidomain, basal lamina protein that plays a key role in the formation and maintenance of the vertebrate neuromuscular junction (Ruegg and Bixby, 1998). Like other extracellular matrix (ECM) molecules, agrin consists of an array of modules homologous to domains found in other ECM proteins.

The amino acid sequence of agrin encodes a protein with a molecular weight (Mw) of 225 kDa, yet, SDS-polyacrylamide gel electrophoresis (SDS-PAGE) analysis shows a diffuse smear around 400 kDa, indicating extensive glycosylation. Treatment with heparitinase or nitrous acid shifts the 400 kDa smear to a focused band of approximately 250 kDa showing that agrin belongs to the family of heparan sulfate proteoglycans (HSPGs) (Gesemann *et al.*, 1995; Hagen *et al.*, 1993). Agrin is thought to contain three glycosaminoglycan attachment sites. In addition to the heparan sulfate (HS) sidechains, agrin contains two serine/threonine-rich regions where O-glycosylation is possible and five potential N-glycosylation sites.

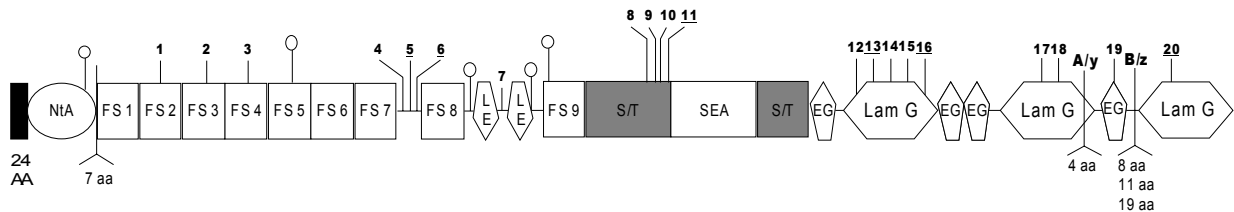


Figure 1 Schematic diagram depicting the domain structure of the agrin core protein. Names and symbols used for the different structural motifs are taken from Bork and Bairoch (Bork and Bairoch, 1995). If the second LG-like domain contains the four amino acid insert at splice site A/y it binds to heparin and the third LG-like domain in conjunction with the B/z site is sufficient to induce aggregation of acetylcholine receptor (AchR) on cultured myotubes. High-affinity binding to α -dystroglycan is observed with an agrin fragment that lacks the AchR aggregation domain and comprises all EGF-like repeats and the first two LG-like domains. Importantly, only those agrin isoforms that have amino acid insert at the B/z site are highly active in aggregation of AchR. The SGs as potential attachment sites for glycosaminoglycans are numbered from 1 to 20; the SGs within a more defined SGXG consensus sequence are underlined. Abbreviations for the domains: NtA: N-terminal agrin domain, FS: follistatin-like domains; LE: Laminin EGF-like module; S/T: serine/threonine-rich domain; SEA: module first found in sea urchin sperm protein; EG: EGF-like domain; Lam G (LG): Laminin G-like domain. The three splice sites of agrin are also indicated.

1. Introduction

The amino-terminus of agrin contains a signal-sequence necessary for its release into the secretory pathway and the N-terminal agrin (NtA) domain, which provides binding to basement membrane-associated laminins via laminin- γ 1 chains (Denzer *et al.*, 1997; Kammerer *et al.*, 1999). The NtA-domain-containing form of agrin is expressed mainly in nonneuronal cells or in neurons that project to nonneuronal cells, for example motor neurons. An alternative form of agrin lacks the NtA-domain but instead encodes a 49 amino acid N-terminus, which converts agrin into a type II transmembrane protein. This form is expressed mainly in neurons of the central nervous system (Burgess *et al.*, 2000; Neumann *et al.*, 2001). Within the N-terminal part of agrin there are nine follistatin-like domains which have been implicated in protease resistance (Biroc *et al.*, 1993) and growth factor binding (Patthy and Nikolics, 1993). The carboxy-terminal part of agrin was shown to be important for its synaptogenic activity. It is sufficient to induce the formation of postsynaptic specializations including aggregates of acetylcholine receptors (AChRs) on cultured myotubes *in vitro* (Nitkin *et al.*, 1987; Reist *et al.*, 1992). The induction of the synapse between nerve and muscle is initiated by the binding of the neuron-specific form of agrin (B/z-isoform) to receptors on the surface of myotubes. Agrin activates a signaling complex that includes the muscle-specific kinase (Musk) and other unidentified components. Musk-receptor activation alone leads to the aggregation of AChR and other proteins of the postsynaptic apparatus. Epidermal growth factor-like (EG) and three laminin G-like (LamG; LG) modules are found within the C-terminal part of agrin. While LG3 is responsible for AChR-clustering, LG2 has been shown to bind to α -dystroglycan. This interaction is not necessary for acetylcholine receptor clustering however, because elimination of the LG2-domain does not reduce agrin's AChR-clustering activity (Gesemann *et al.*, 1996; Hopf and Hoch, 1996).

Targeted inactivation of agrin in mice results in grossly malformed neuromuscular junctions (NMJs), which display very few pre- and postsynaptic specializations. These mice die at birth because of insufficient activation of respiratory musculature (Gautam *et al.*, 1996).

Agrin cDNA is highly homologous throughout the examined species (rat, chick, marine ray, and human), and the domain structure of the deduced protein is highly conserved.

1. Introduction

The agrin gene is subject to alternative mRNA splicing at several sites. Alternative exon usage at positions A and B (called y and z in rodents) at the 3' end of the cDNA has a strong influence on the biological activity of agrin. Only those isoforms which have a peptide insert in both sites are capable of inducing AchR clustering at the NMJ *in vitro* and *in vivo* (Burgess *et al.*, 1999; Cohen *et al.*, 1997a; Ferns *et al.*, 1993; Gesemann *et al.*, 1995; Ruegg *et al.*, 1992). So far only neurons, specifically motor neurons, have been shown to express agrin isoforms that contain B/z inserts. The agrin isoforms expressed in other tissues such as lung and kidney lack inserts at the B/z site. Because these isoforms lack the clustering activity, but still bind with high affinity to α -dystroglycan, it is possible they function as adhesive molecules between cells and the ECM.

Agrin isoforms containing the B/z-insertion are able to induce the phosphorylation of the transcription factor cAMP response element binding protein (CREB) in primary hippocampal neurons (Ji *et al.*, 1998).

Agrin binds to a number of known heparin-binding proteins *in vitro* via its glycosaminoglycan-chains (e.g. FGF-2 and thrombospondin) or via its core-protein (e.g. laminin-1, merosin and tenascin) (Cotman *et al.*, 1999; Denzer *et al.*, 1998). Previous studies using electron microscopy showed a 90 nm distance between the NtA-domain that binds to laminin and the last LG domain which was shown to be sufficient to induce AchR aggregation (Gesemann *et al.*, 1995).

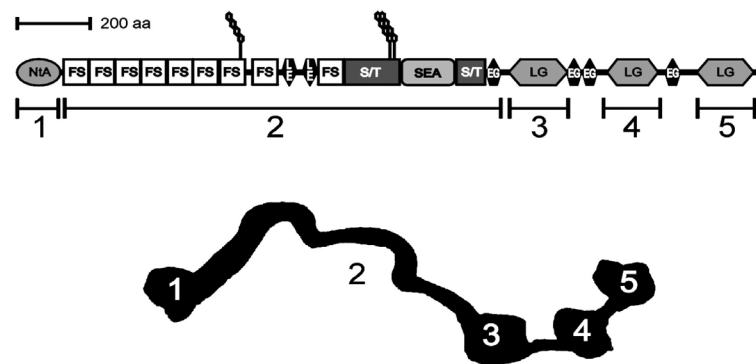


Figure 2 Alignment of the domains of agrin to the structure of agrin. The schematic representation of the domain organization of agrin and the structure of a selected electron micrograph of agrin are shown. For symbols and designations of individual domains, see Figure 1 (picture taken from: Denzer *et al.*, 1998).

The length of agrin is therefore sufficient to span the entire basal lamina, which is ~50 nm between the presynaptic nerve terminal and the postsynaptic muscle fiber.

Furthermore, agrin has been shown to be a major component of senile plaques in dementia of the Alzheimer's type (Donahue *et al.*, 1999). By using solid-phase immunoassay, an interaction between agrin and the amyloidogenic peptide A β (1-40) in its fibrillar state was shown. This mechanism is GAG chain dependent, as this interaction was prevented after agrin was treated with heparitinase. In addition, agrin accelerates A β fibril formation and contributes to larger fibrils than control samples, *in vitro*. Furthermore, agrin protects protein aggregates from proteolytic degradation *in vitro* most likely mediated through its protease inhibitor domains (Cotman *et al.*, 2000).

1.1 Binding to laminin-1

Agrin was shown previously to bind laminin-1 via its N-terminal agrin (NtA)-domain which comprises the first 135 amino acids of agrin (Denzer *et al.*, 1997). Members of the laminin family are principle components of basement membranes. Laminins are heterotrimers consisting of α , β and γ subunits which are interlinked by an extensive coiled-coil domain, forming the long arm of the cruciform shaped molecule (Beck *et al.*, 1990; Maurer and Engel, 1996; Timpl and Brown, 1994; Timpl and Brown, 1996).

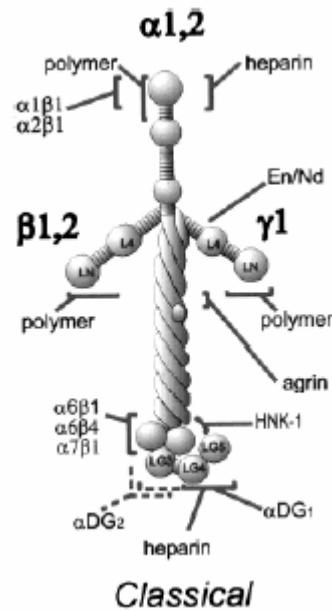


Figure 3 Laminin heterotrimer morphologies and functions. Each laminin is a heterotrimer composed of an α , β and γ chain subunit joined together in parallel in a coiled-coiled. Although most trimeric combinations are allowed, the $\gamma 2$ chain and $\beta 3$ chains are found only in association with each other and with the $\alpha 3$ -chain. Polymerization (self-assembly) sites have been assigned to the LN domains, possibly requiring the participation of more distal domains. The nidogen/entactin-binding site lies within $\gamma 1$ (III)-repeat. Heparin binding sites are found in the α -chain in both G-domain (major) and the N-terminal LN domain (minor). α -dystroglycan (αDG) binds to fragment E3 of laminin, corresponding to G4/G5 in laminin-1. Agrin binds to the coiled-coil through a conformation-dependent interaction mediated largely through the $\gamma 1$ chain (picture taken from: Colognato and Yurchenco, 2000).

Laminins are known to bind to various $\beta 1$ and $\beta 4$ integrins, dystroglycan, a receptor tyrosine phosphatase, heparan sulfates, and other cell surface proteins. Agrin binds to the central region of the three-stranded coiled-coil oligomerization domain in the long arm of laminin-1, which mediates subunit assembly of the native laminin molecule. By a combination of electron microscopy and mutational analysis, the binding site of laminin to the NtA was localized in the central region of the about 60 nm long arm of laminin-1. The agrin-binding site in laminin maps to 20 residues within the $\gamma 1$ -chain of laminin and requires the native coiled-coil conformation for binding to agrin (Kammerer *et al.*, 1999). Sequences of the chains exhibit the typical heptad repeat $(abcdefg)_n$ of coiled-coil structures in which residues in position a and d are restricted to the core, while residues in other positions are usually of charged and polar nature and are exposed to the surface (Cohen and Parry, 1990).

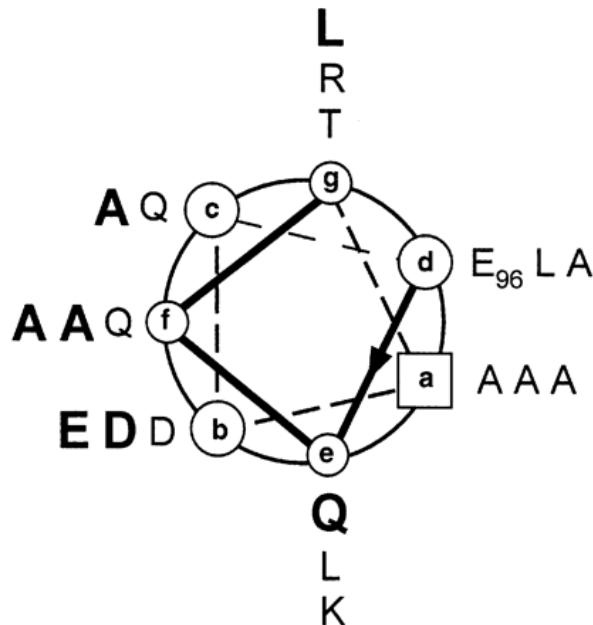


Figure 4 Helical wheel representation of residues comprising the agrin-binding site. The sequence starts with Glu₉₆ (Glu₁₂₉₆; (Sasaki and Yamada, 1987)) in a heptad **d** position and ends with Glu₁₁₅ (Glu₁₃₁₅) in a heptad **b** position. View is from the N-terminus, and heptad repeat positions are labeled **a-g**. The seven surface-exposed residues of the $\gamma 1$ chain that are not conserved in the $\gamma 2$ chain are indicated in bold (picture taken from: Kammerer *et al.*, 1999).

Because hydrophobic amino acids tend to be oriented towards the center of the superhelix, the negatively charged amino acids in position **b** are facing the outside and are therefore available for ionic interactions. Thus, positively charged amino acids within the NtA-domain of agrin are likely counterparts and could mediate binding. Site-directed mutagenesis of positively charged amino acids can be therefore a suitable method to identify amino acids involved in the binding mechanism, or required for the correct formation of the binding site. Through comparison of human, mouse, and chick protein sequences, highly conserved positively charged amino acids were identified and chosen for site-directed mutagenesis.

The X-ray structure of the chicken NtA-domain at 1.6 Å resolution revealed a β -barrel fold flanked by α -helices at both termini which are characterized by a high content of charged amino acids (Stetefeld *et al.*, 2001).

1. Introduction

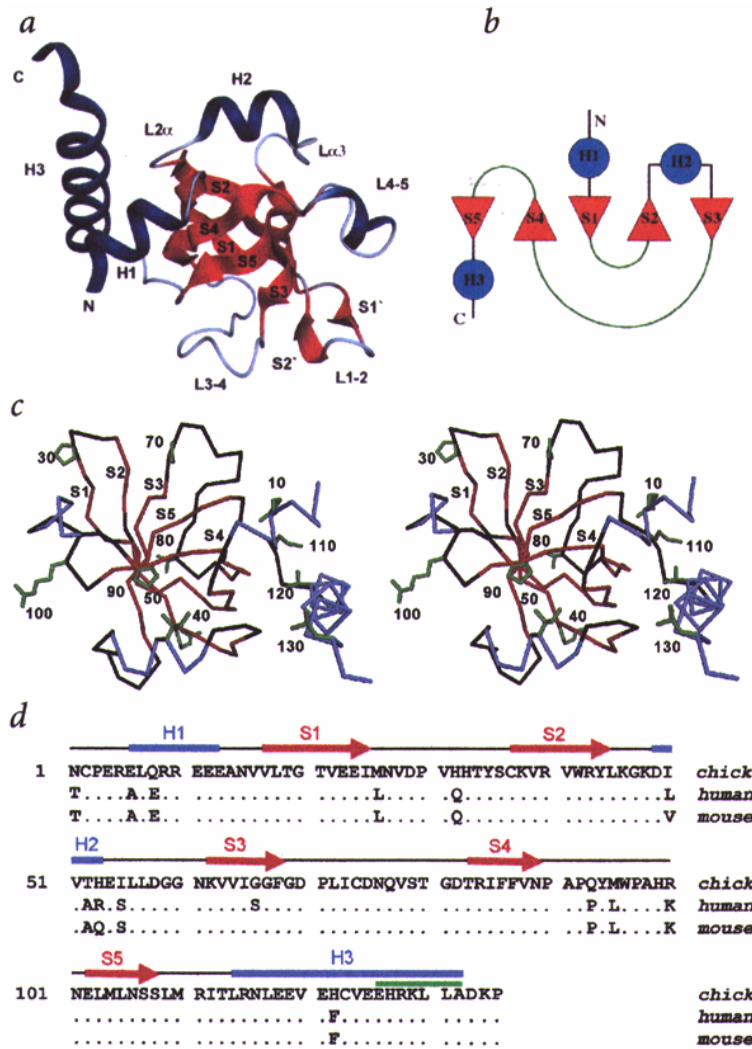


Figure 5 Structure of the NtA-domain. **a**, Ribbon diagram of the NtA structure. β -strands are in red and labeled sequentially from S1 to S5. α -helices (H1–H3) and the 3_{10} -helix in loop L4–5 are in blue. The loops connecting strands S1 and S2 (L1–2), strands S3 and S4 (L3–4), and strands S4 and S5 (L4–5) are oriented to the same surface of the protein. **b**, Topology diagram of the secondary structural elements. Red arrows represent β -strands, and blue circles depict α -helices. Connections representing loop regions L1–2, L3–4 and L4–5 are shown as green lines. All other connections are shown as black lines. **c**, Stereo $C\alpha$ trace with every 10th residue labeled. **d**, Alignment of known NtA sequences. Sequences are shown as blocks of ten residues, and conserved residues are indicated by dots. Sequence numbers correspond to the mature protein. Secondary structure elements are indicated above the alignment using the same color code as in (a). Helix H3 contains a splice insert, residues Glu 126–Ala 132 (highlighted by the green bar), whose function is yet unknown. All figures have been prepared using the program DINO (<http://www.biozentrum.unibas.ch/~xray/dino/>) (Stetefeld *et al.*, 2001).

The C-terminal α -helix (helix 3) contains a 7-residue splice insert comprised of residues E126–A132, with yet unknown function. Motor neurons in developing spinal cord contain agrin transcripts that include this splice insert. However, the majority of agrin mRNA in

1. Introduction

non-neuronal tissue is characterized by the absence of the 7-residue insert (Denzer *et al.*, 1995; Tsen *et al.*, 1995).

The expressed proteins were purified as described, and their ability to bind laminin-1 was determined by a solid phase binding assay. An unmutated agrin fragment consisting of the NtA- and 1. Follistatin (FS)-domain, previously described to be sufficient for laminin-1 binding (Denzer *et al.*, 1997), was used as a control. To verify the results obtained *in vitro*, the binding of agrin and laminin were confirmed by *in vivo* experiments testing the integration of the NtA-domain into basal lamina.

1.2 Fusion protein with NGF

The autocrine/paracrine peptide signaling molecules such as growth factors have many biologic activities promising for clinical application. Unfortunately, most drug delivery systems are not suitable for clinical application with growth factors because of their limited target specificity and short half lives *in vivo*.

To overcome the problem of target specificity, studies have been conducted trying to develop novel drug delivery systems that enable the factors to act on restricted target cells. A fusion protein from epidermal growth factor (EGF) and the cell-binding domain of fibronectin exhibited both cell-adhesive activity and growth factor activity, each of which was indistinguishable from that of the corresponding, unfused protein (Kawase *et al.*, 1992). In a different approach EGF was immobilized on a modified glass surface via star poly-(ethylene oxide) (PEO) (Kuhl and Griffith-Cima, 1996). The flexible PEO arms permitted the EGF molecule to retain its native conformation and to interact with its receptor in a relatively unrestricted manner. As a result, the immobilized EGF (tethered EGF) showed biologic activities comparable with those of soluble EGF *in vitro*. In such studies, however, the limited capacity of the cell surface receptors to retain the fusion protein (C-EGF) or the use of artificial matrices (tethered EGF) may be a problem for clinical applications.

In a more recent study fusion proteins consisting of the collagen-binding domain (CBD) derived from *clostridium histolyticum* collagenase and growth factor moieties showed that the CBD can be used as an anchoring unit, preventing the diffusion of the peptide and hence increase its timely presence at a specific site. Another study utilized a fusion protein of biologically active EGF and the fibronectin collagen-binding domain (Ishikawa *et al.*, 2001). This fusion protein substantially stimulated cell growth *in vitro* and showed wound healing inducing properties *in vivo*.

The present study was aimed at creating a fusion protein that would be able to bind to laminin while still displaying properties of the nerve growth factor (NGF). NGF is a member of the neurotrophin protein family that promotes the survival, growth and maintenance of neurons in the central and peripheral nervous system. *In vivo* NGF is

produced as a pre-pro-protein (Berger and Shooter, 1977; Ullrich *et al.*, 1983). The 18 amino acid pre-sequence is cleaved off when the protein is translocated into the endoplasmatic reticulum. The pro-sequence (103 amino acids) is thought to play a crucial role either in the folding of the mature protein, or its secretion out of the cell. The biologically active NGF-mature is a homodimer consisting of 118 amino acids per monomer.

The advantage of using NGF in this study is its already well defined biological activity that can be demonstrated in neurite outgrowth assays. In this study NtA-domain containing protein fragments (PF5 and PF8) were fused to NGF-mature. The purified proteins were tested *in vitro* and *in vivo* for their laminin-binding ability and the biological activity of the fused NGF-moiety.

1.3 Glycosylation of agrin

Proteoglycans (PGs) are proteins with long glycosaminoglycans (GAGs) attached to a core protein. They are predominantly found in the extracellular matrix and connective tissues and influence a variety of cellular and physiological activities including cell proliferation, cell adhesion, blood coagulation, and wound repair (Kjellen and Lindahl, 1991). Approximately 30 PG core proteins have been identified with sizes ranging from 10 to >500 kDa and the number of attached GAG chains ranging from 1 to >100. The most abundant GAGs are heparan sulfate (HS) and chondroitin sulfate (CS). HS and CS are synthesized via similar routes involving the stepwise addition of four monosaccharides to serine residues.

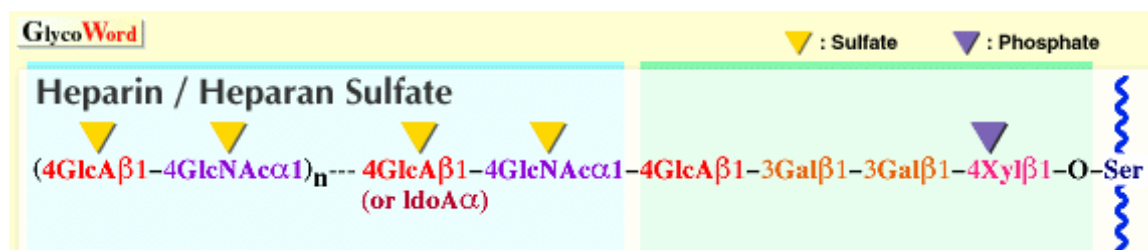


Figure 6 Glycosaminoglycan structure (taken from the website: <http://www.glycoforum.gr.jp/science/word/proteoglycan/PGA06E.html>)

It has been shown that serine followed by glycine residues are heavily favored acceptors for xylosyltransferase (Roden *et al.*, 1985), the key enzyme in the initial step of GAG glycosylation.

The information for priming of GAG synthesis as well as determining the type of glycosylation has to be encoded in the core-protein sequence itself, because cells that are capable of generating both kinds of GAGs reliably put the correct carbohydrates onto a defined core protein. The formation of HS for example, is enhanced when the core protein sequence contained two or more serine-glycine (SG)-consensus sequences in close proximity to each other, a cluster of acidic amino acids nearby, and a tryptophan residue immediately followed a (SG)-GAG attachment site (Dolan *et al.*, 1997; Zhang *et al.*, 1995; Zhang and Esko, 1994). However, acidic clusters are also found in CSPGs (Bourdon *et al.*, 1987; Brinkmann *et al.*, 1997) and thus seem to be necessary but not sufficient for the formation of HS. Better knowledge of glycosylation sites of PGs would help to define the rule of glycosylation more clearly.

While the GAG attachment sites of perlecan (Dolan *et al.*, 1997), collagen XVIII (Dong *et al.*, 2002) and syndecan have been determined (Zhang *et al.*, 1995), the sites in agrin are still unknown. In the present study, the potential (SG) sites were examined for GAG priming activity by expressing peptide fragments in eucaryotic cells and analyzing the recombinant products for glycosylation.

1.4 Neurite outgrowth inhibition by agrin

While the influence of agrin on postsynaptic differentiation was subject to a number of studies, recent experiments have revealed that agrin might work as a “stop-signal” for axons from presynaptic neurons. It is known that agrin directly acts on neurons, which may be important for the development of the central nervous system as well as for the differentiation of the NMJ. *In vitro*, agrin was shown to inhibit neurite growth and initiate vesicle clustering (Campagna *et al.*, 1995; Campagna *et al.*, 1997; Chang *et al.*, 1997; Halfter *et al.*, 1997). Previous studies revealed that the interaction of agrin with laminin-1 has no influence on the neurite inhibition of agrin, because inhibition was shown for

neurite growth induced by laminin-2 (Halfter *et al.*, 1997), laminin-1 and N-cadherin (Bixby *et al.*, 2002).

Because agrin is expressed throughout the central nervous system, it seems likely that agrin's effect on neurons is not limited to the NMJ (Cohen *et al.*, 1997b; Halfter *et al.*, 1997; Ma *et al.*, 1994; O'Connor *et al.*, 1994). It was reported that full-length agrin, as well as a N-terminal 150 kDa fragment of agrin inhibited neuron outgrowth of ciliary ganglia (CG) neurons *in vitro*, while a C-terminal 95 kDa fragment had no influence on neurite outgrowth (Bixby *et al.*, 2002). These findings imply that the N-terminal domains of agrin are responsible for this effect. In the present study various fragments of the N-terminal domains of agrin were tested for their inhibitory effect on neurite outgrowth. To test the influence of GAG chains in this matter, fragments containing GAG chains, as well as mutants of the same fragments without GAG chains were tested in a neurite outgrowth assay utilizing dorsal root ganglia (DRG).

1.5 The episomal expression system in human embryonic kidney cells (HEK) and choice of Tag module

This system, based on the expression vector pCEP-Pu and HEK293/EBNA cells (Invitrogen, Carlsbad, CA), has been used successfully in the expression of many extracellular proteins. In this case, the genome of the human embryonic kidney cells carries the EBNA-1 gene of the Epstein-Barr Virus (EBV), as well as a resistance to the selection marker G 418 (Geneticin).

The vector used in these studies, is a modified version of the episomal expression vector pCEP (Invitrogen). The original vector contains the EBNA-1 gene (Epstein-Barr nuclear antigen 1), which encodes a viral DNA binding protein essential for the extra chromosomal existence of the plasmid. Another component of the vector is the EBV-replication origin, oriP, which is essential for a high vector replication rate independent of proliferation. The interaction of EBNA-1 with oriP plays an important role in DNA replication and the stable distribution of the episomal vectors in dividing cells.

1. Introduction

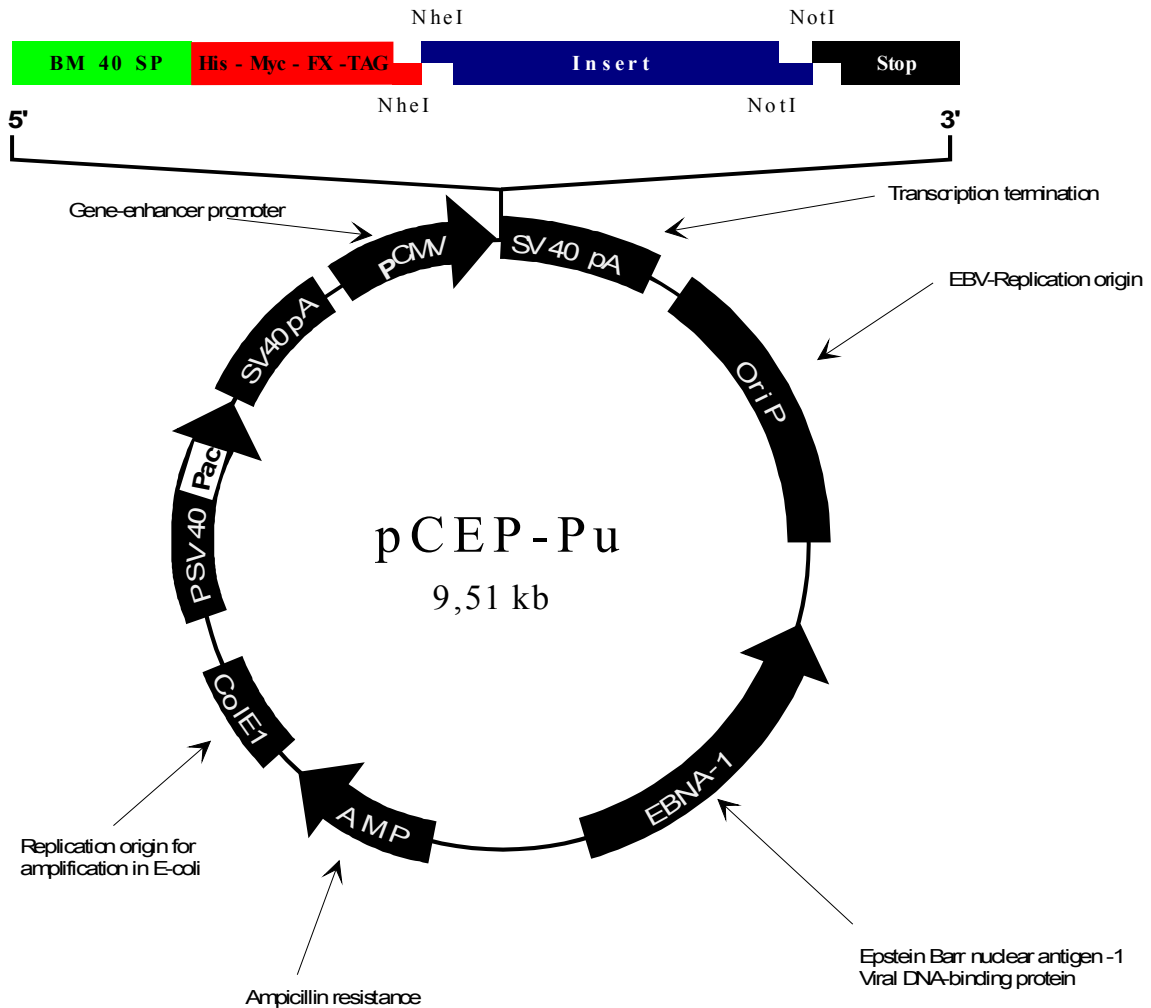


Figure 7 Modified version of the expression vector pCEP-Pu ((Kohfeldt *et al.*, 1997), kindly provided by Prof.Dr. Mats Paulsson, Cologne, Germany)

The EBNA-1 gene is present in the genome of the HEK293-cells as well as in the expression vector to ensure a high protein expression. The vector also contains genes necessary for the amplification in E.Coli, such as the ColE1 replication origin and an ampicillin resistance gene. To stimulate high recombinant protein expression the CMV-promoter (human cytomegalovirus immediate-early gene enhancer-promoter) is included as part of the vector. cDNA fragments can be inserted into a multiple cloning site, which is followed by a polyadenylation site and the SV40 transcription terminator. The modified vector contains a puromycin-resistance cassette instead of a hygromycin-resistance gene (pCEP-Pu) (Kohfeldt *et al.*, 1997), and the BM40 signal peptide was added, which is sufficient for the secretion of the recombinant protein from the cell.

1. Introduction

In order to analyze recombinant protein, it is essential to obtain the purest samples possible. One way to achieve this is to express the protein as a fusion protein with a module that has already been proven to be effective in affinity purification of proteins (Ford *et al.*, 1991; Sherwood, 1991).

The choice of module can vary between whole proteins to stretches of 6-10 amino acids. High affinity modules have the drawback of sometimes needing non physiological conditions to elute the protein which can lead to denaturation. Larger tags will always bind to the affinity column because they cannot be incorporated inside the protein during the folding process, which might be a problem with smaller tags. Larger tags, however, usually have an impact on the folding ability of the protein and hence alter its properties. These tags must then be removed with proteases before use of the protein. Small tags usually have a negligible influence on protein folding, although occasional interferences can occur (Ledent *et al.*, 1997). In the performed experiments, all proteins were expressed as fusion proteins with an N-terminal His₆-Myc-FactorX-Tag as well as a BM-40 signalpeptide necessary for the release of the protein into the cell supernatant.

MRAWIFFLLCLAGRALA:APLV	BM-40 Signalpeptide
HHHHHH	His ₆
GPLVDVASN	
EQKLISEEDL	Myc-sequence
ASMTGGQQMGRD	
IEGRG	Factor-X sequence
LA	

The cutting site for the BM-40 signalsequence was being determined by using the SignalP V1.1 World Wide Web Server (<http://www.cbs.dtu.dk/services/SignalP/>) and is most likely positioned between alanine (17) and alanine (18). The remaining 48 amino acids of this tag encode for a 5.18 kDa peptide, determined using the ProtParamTool World Wide Web Server (<http://us.expasy.org/tools/protparam.html>).

1. Introduction

The His₆-Tag allows purification of the expressed proteins from cell supernatant by affinity chromatography using a commercially available purification system. Talon[®] resins (Clontech/BD Biosciences, Palo Alto, CA) are cobalt-based IMAC (Immobilized Metal Affinity chromatography) resins designed to purify recombinant polyhistidine-tagged proteins (Bush *et al.*, 1991). Talon[®] utilizes special tetradentate metal chelator for purifying the tagged proteins. The binding pocket is an octahedral structure in which four of the six metal coordination sites are occupied by the Talon[®] ligand.

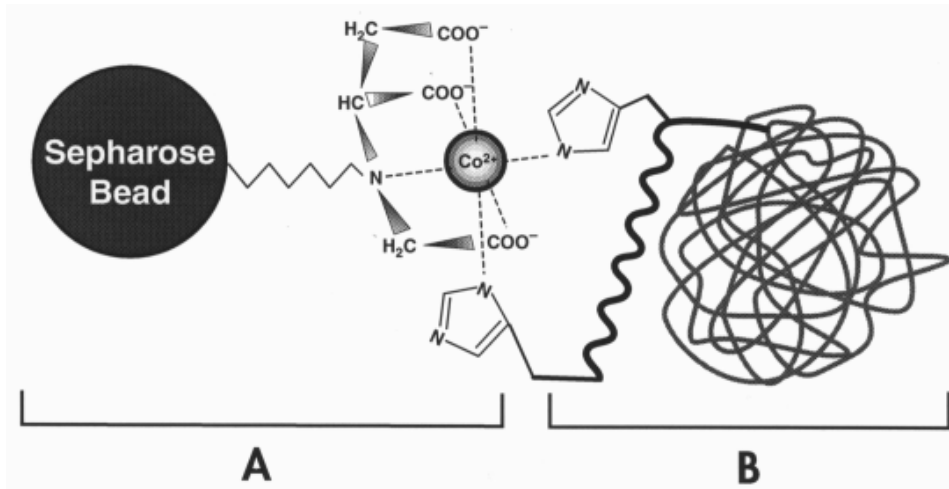


Figure 8 Schematic diagram of the TALON™ IMAC System. Part A. TALON™ Metal Affinity Resin; A Sephadex bead bearing the tetradentate chelator of the Co²⁺ metal ion. Part B. The polyhistidine-tagged recombinant protein binds to the resin (Clontech, 2002).

The Myc-Tag (EQKLISEEDL) allows the detection of the protein with a highly specific mouse monoclonal IgG antibody (c-Myc (9E10):sc-40; Santa Cruz Biotechnology, Santa Cruz, CA). FactorX (IEGRG) is a protease restriction site, which allows removal of the tag in case it should interfere with one of the experiments.

1.6 Aim of the project

While the C-terminal domains of agrin have been the subject of a number of studies, very little is known about the N-terminal domains of agrin which account for almost 2/3 of the protein. The goal of this project was to elucidate some of the functions for these N-terminal domains. These include

1. examination of the binding mechanism of the laminin-binding site of agrin
2. localization of the GAG attachment sites in the core protein
3. neurite outgrowth inhibition of agrin

To accomplish this, 9 N-terminal fragments of agrin, expressed in an eucaryotic expression system were the subject of *in vitro* and *in vivo* binding studies, site-directed mutagenesis experiments and neurite outgrowth assays.

2. Methods and Materials

2. Chemicals

If not specifically stated, all chemicals were ordered from Sigma, Invitrogen, or Fluka. Enzymes were purchased from New England Biolabs or Promega.

Cell culture media and chemicals were obtained from Cellgro, Sigma, Gibco, and Bio-Whittaker.

Purified water was produced by a Millipore system (Millipore QF, Millipore Corp., Bedford, MA)

2.1 Molecular Biology

2.1.1 PCR

Plasmid MC1061/P3 (Invitrogen, Carlsbad, CA) containing full-length chick agrin cDNA was used as the template to generate the different agrin fragments.

The following protocol was used to generate constructs PF1-PF9:

To 100 ng plasmid in 15 μ l H₂O

Add	2 μ l 10x cloned Pfu DNA polymerase reaction buffer
	1 μ l dNTP's (25 mM each dNTP)
	1 μ l Sense-Primer (100 ng/ μ l)
	1 μ l Anti-Sense-Primer (100 ng/ μ l)
	0.4 μ l PfuTurbo DNA polymerase (2.5 U/ μ l)

The following primers were used to generate constructs PF1-PF9:

PF1

S: 5'-GTCAGCTAGC(T)AACTGCCCCGAACGGGA-3'

AS: 5'-TTCTTCTTCAGCGGCCGCGTACTGAGGGGCTGGGTTGA-3'

2. Materials and Methods

PF2

S: 5'-GTCAGCTAGC(T)ATGTGGCCTGCCACCGCAA-3'

AS: 5'-TTCTTCTTCAGCGGCCGCGGTGAGGCCATCGGTGCCACA-3'

PF3

S: 5'-GTCAGCTAGC(T)CAGTGCGTGTGTCCCCGCTGT-3'

AS: 5'-TTCTTCTTCAGCGGCCGCGCTCCCTTCTGCATCAGCA-3'

PF4

S: 5'-GTCAGCTAGC(T)AACTGTCCGGCTACCAAAGTC-3'

AS: 5'-TTCTTCTTCAGCGGCCGCGGCCAGGTAGGACTTGCCA-3'

PF5

S: 5'-GTCAGCTAGC(T)AACTGCCCCGAACGGGA-3'

As: 5'-TTCTTCTTCAGCGGCCGCCACCTCTGCACAGGGGT-3'

PF6

S: 5'-GTCAGCTAGC(T)AAGGACCCCTGTGCAGAGGTG-3'

AS: 5'-TTCTTCTTCAGCGGCCGCCTGACTGCAGTGCACA ACTGG-3'

PF7

S: 5'-GTCAGCTAGC(T)CCAGTTGTGCACTGCAGTCAG-3'

AS: 5'-TTCTTCTTCAGCGGCCGCGCTCCCTTCTGCATCAGCA-3'

PF8

S: 5'-GTCAGCTAGC(T)AACTGCCCCGAACGGGA-3'

AS: 5'-TTCTTCTTCAGCGGCCGCGGAGGCTTGGGAGGGGT-3'

PF9

S: 5'-GTCAGCTAGC(T)TCCCAAGCCTCCTGTGTCTGC-3'

AS: 5'-TTCTTCTTCAGCGGCCGCCTGACTGCAGTGCACA ACTGG-3'

NGF-mature

NGF-S: 5'-TTCTTCTTCA GCGGCCGCT AAG CGC TCA TCC ACC C-3'

NGF-AS: 5'-TTCTTCTTCA GCGGCCGC GCC TCT TCT TGT AGC CT-3'

The primers were designed to introduce terminal NheI and NotI restriction sites to the fragments. These fragments were then cloned into the pCEP-Pu/EBNA-vector in frame with the BM-40 signal peptide and an N-terminal His₆-Myc-FactorX-Tag.

2. Materials and Methods

Primers containing an NheI cutting site were protected by 4 nucleotides at the 5' end and contained an additional "T" directly following the cutting site, to keep the insert in frame with the preceding tag-module. Primers containing a NotI cutting site were supplemented with 10 additional nucleotides at the 5' end to achieve optimal cutting efficiency.

In the case of NGF-mature, full-length NGF in a Bluescript-vector was used as the template to generate cDNA encoding NGF-mature (366 bp). Primers were designed to introduce terminal NotI restriction sites to the fragment. Because the 5'-end and the 3'-end contain the same restriction site, ligation into the NotI-cut vector generated two different products. The correct insert orientation was verified by sequencing.

Program used for generating the different PCR constructs:

Step	Repeats	Temperature	Time
1	1	95°C	2'
2	30	95°C PrimerTm - 5°C 72°C	30'' 30'' 1' per kb for targets < 10kb 2' per kb for targets > 10kb
3	1	72°C	10'

2.1.2 Site-directed mutagenesis

The cDNAs of fragments PF7 and PF9 in pCEP-Pu/EBNA were used for site-directed mutagenesis experiments to determine the location of the SG consensus sequences for GAG glycosylation. The cDNA of PF5 in pCEP-Pu/EBNA was used for site-directed mutagenesis experiments to investigate the laminin-binding site of agrin. Single point mutations were introduced by designing primers according to the Quick Change site-directed mutagenesis kit (Stratagene, La Jolla, CA) user's manual. Multiple point mutations were introduced by additional site-directed mutagenesis on single and double-mutant cDNAs. The following oligonucleotides were used to introduce mutations

2. Materials and Methods

(mutated bases are shown in lower case letters): only the sense-primers are shown below. Antisense-primers were the inverted and complementary oligonucleotides.

Primers used for glycosylation studies:

M 4: 5'- GGA CGA ATG TGG CgC AGG GGG CTC AGG CTC TGG -3'

M 5: 5'- GTG GCT CAG GGG GCg CAG GCT CTG GTG ATG GG -3'

M 6: 5'- CAG GGG GCT CAG GCg CTG GTG ATG GGA GTG AGT G -3'

M 4+5: 5'- GTG GCg CAG GGG GCg CAG GCT CTG GTG ATG GG -3'

M 5+6: 5'- CAG GGG GCg CAG GCg CTG GTG ATG GGA GTG AGT G -3'

M 8: 5'- GCC TCC CTA CGC TGA AgC GGG Cgc TGC AGA AGG C -3'

M 9: 5'- GCA GTG CAG AAG GCg cTG GGG ACC AGG AGA TGA GC -3'

M 10: 5'- CCA GGA GAT GAG CAT Cgc TGG GGA CCA GGA ATC C -3'

M 10c: 5'- CCA GGA GAT GAG CAT Cgc TGG GGA CCA GGA AgC C -3'

M 11: 5'- GGA CCA GGA AgC Cgc TGG GGC AGG CgC TGC TGG GGA AGA G -3'

Primers used for laminin-binding studies:

M 5: 5'- GCT AAC TGC CCC GAA gcG GAG CTG CAG-3'

M9,10: 5'- AAC GGG AGC TGC AGg cCg cGG AGG AGG CCA AC -3'

M 43: 5'- GGT GAG AGT GTG Ggc TTA CCT GAA AGG C-3'

M 84: 5'- CGA CCG GGG ACA CAg cGA TAT TCT TTG TCA ACC CAG CCC-3'

M 111: 5'- CAA CTC CAG CCT GAT Ggc GAT CAC GCT GCG CAA C-3'

M 115: 5'- GAT GCG GAT CAC GCT Ggc CAA CCT GGA GGA GGT G-3'

M 128,129: 5'- GCG TGG AAG AAC ATg cGg cGC TTC TTG CTG ACA AG-3'

All sequences were verified by sequencing in the universities sequencing facility. The sequences were analyzed using the Sequencher-Software (DNA Codes Inc., Ann Arbor, MI). Amino acid sequences were deduced from the DNA sequences using the same software.

2. Materials and Methods

Protocol for site-directed mutagenesis according to the manufacturers recommendation:

- 1 μ l DNA (25-50 ng/ μ l)
- 2 μ l 10x Reaction Buffer
- 0.25 μ l Sense-Primer (10 μ M)
- 0.25 μ l Antisense-Primer (10 μ M)
- 1 μ l dNTP (10 mM)
- 15.5 μ l H₂O
- 0.4 μ l Pfu-Turbo

The following program was used in a single-block thermocycler:

Step	Repeats	Temperature	Time
1	1	95°C	30''
2	18	95°C	30''
		55°C	1'
		68°C	2' per kb target DNA
3	1	68°C	10'

2.1.3 Agarose gel electrophoresis

For the performed experiments, a 1% agarose gel was used.

For this purpose 0.5 g agarose was heated in 50 ml TAE-buffer, and ethidiumbromide was added to a final concentration of 0.5 μ g/ml. After polymerization, the gel was transferred to an electrophoresis gel-chamber and submerged in TAE-buffer. The samples were mixed with Gel Loading Solution (Sigma, St. Louis, MO) and loaded into the gel. The Ready-Load™1 kb DNA Ladder (Invitrogen, Carlsbad, CA) or the EZ-Load™1 kb Molecular Ruler (Bio-Rad, Hercules, CA) was used as molecular weight standard, depending on the expected DNA size. Electrophoresis was carried out at constant voltage that did not exceed 5 V/cm Gel-length.

2. Materials and Methods

2.1.4 DNA gel elution

Elution from DNA-fragments from agarose gels was performed by using the Qiaex[®] II-Gel extraction Kit from Qiagen (Qiagen, Valencia, CA) according to the manufacturer's recommendations.

2.1.5 Endonuclease digestion

Protocol for digestions with 2 restriction enzymes:

1 µg DNA

2 µl 10x Restriction Buffer

0.2 µl BSA (100x)

2-5 U Enzyme 1

2-5 U Enzyme 2

Incubation occurred at 37°C for at least 1 hour.

2.1.6 DNA quantification

To determine the concentration of a given DNA sample, the optical density of the DNA sample was measured at 260 and 280 nm with a UV-Spectrometer. To verify the purity of the sample, the ratio of OD260 to OD280 was calculated.

2.1.7 Dephosphorylation

After restriction digestion, the solution was heated to 65°C for 20 minutes to inactivate the restriction enzymes.

To prevent religation of linearized vector-DNA, it was treated with alkaline phosphatase (from calf intestine; Roche, Indianapolis, IN) to remove the 5'-phosphates of the DNA.

10 µl DNA (cut)

0.9 µl 10x Buffer

1 µl SAP (= 1 U)

2. Materials and Methods

Incubation was carried out for 1 hour at 37°C. The preparation was then purified by agarose gel electrophoresis using 1% agarose. The desired bands were excised, and the DNA was eluted from the gel using the Qiaex[®] II-Gel extraction Kit from Qiagen according to the manufacturer's recommendations.

2.1.8 Ligation

5x pmol Insert

x pmol Vector

1 µl 10x T4-Ligase Buffer

1 µl T4-Ligase

The ligation of linearized, dephosphorylated vector and double stranded PCR fragment that have been cut with the same restriction enzymes, was performed over night at 14°C. T4 Ligase catalyzes the reaction between the 5' phosphate- of the DNA insert and the 3' hydroxyl- group of the vector to form a phosphodiester bond.

2.1.9 Production of competent bacteria

500 ml of LB medium was inoculated with 5 ml overnight bacteria culture. The solution was shaken at 37°C until it reached an OD₅₉₅ of 0.4-0.7. All of the following steps were performed on ice. The solution was cooled for 15 minutes and then centrifuged at 3000 g for 10 minutes. The pellet was resuspended in 100 ml TFB I (30 mM KAc pH 5.8, 50 mM MnCl₂, 100 mM RbCl, 10 mM CaCl₂, 15% glycerol (w/v)) and incubated on ice for 10 minutes. Then the solution was centrifuged for 10 minutes at 3000 g. The pellet was resuspended in 20 ml TFB II (10 mM MOPS pH 7.0, 75 mM CaCl₂, 10 mM RbCl, 15% Glycerol (w/v)). The competent bacteria were then stored in 100 µl aliquots at -80°C.

2. Materials and Methods

2.1.10 Bacterial “heat shock” -transformation

Plasmid DNA was transformed into 100 µl XL1-Blue or MC1061/P3 cells by heat shock transformation. 1 ng DNA or 5 µl of the ligation was incubated with bacteria for 20 minutes on ice while mixing the solution every 5 minutes. Afterwards the mixture was placed into a 42°C water-bath for 1 minute and immediately put on ice for 2 minutes. The cells were suspended 900 µl of LB-medium and shaken at 37°C for 1 hour. Then, 200 µl of the solution was plated on plates containing 100 µg/ml ampicillin or plates containing 100 µg/ml tetracycline and incubated overnight at 37°C.

2.1.11 DNA-purification

DNA-purification was performed using the Wizard[®] Plus Miniprep DNA Purification System (Promega, Madison, WI). The Kit was used as recommended in the user’s manual.

2.1.12 Sequencing

All sequences were verified by sequencing in the universities sequencing facility. The DNA Sequencing Core Facility at the University of Pittsburgh utilizes two ABI PRISM[®] 3100 Genetic Analyzers. Each unit incorporates a multi-color fluorescence-based DNA analysis system using the proven technology of capillary electrophoresis with 16 capillaries operating in parallel. The 3100 Genetic Analyzers are fully automated from sample loading to data analysis.

Samples were prepared as followed:

1.5 µg DNA

add H₂O to 12 µl

1 µl Primer (320 pmol/µl) The sequences were analyzed using the Sequencher[™]-Software (DNA Codes Inc., Ann Arbor, MI). Amino acid sequences were deduced from the DNA sequences using the same software.

2.2 Protein biochemistry

2.2.1 SDS gel electrophoresis

Samples were treated with SDS-sample buffer, boiled for 5 minutes and analyzed by SDS-polyacrylamide gel electrophoresis. A 4% upper gel and depending on the sample, 10%, 12% or 3.5-15% gradient gels were used. Gels were run at a constant voltage of 120 V. The prestained SDS-PAGE Standards, Broad Range Marker (BioRad, Hercules, CA) were used as molecular weight standard.

2.2.2 Western blotting

Proteins were transferred to a nitrocellulose membrane (Millipore, Bedford, MA) using a semi-dry blotting system (BioRad, Hercules, CA). Unspecific binding was prevented by incubating the membrane with blocking solution (TBS + 5% dry milk powder) for 30 minutes. The membrane was then incubated for 1 hour with the primary antibody in blocking solution. After three washes with blocking solution, the blot was incubated with the alkaline phosphatase conjugated secondary antibody in blocking solution for 1 hour. The membrane was washed three times with blocking solution and then thoroughly with water. The blot was incubated for 10 minutes in developing buffer (0.1 M Tris, 0.1 M NaCl, 0.05 M MgCl₂). The blot was developed by adding a mix of developing buffer, NBT (4-nitro blue tetrazolium chloride) and BCIP (5-bromo-4-chloro-3-indolyl-phosphate) (Roche, Indianapolis, IN).

2.2.3 Construction, expression and purification of recombinant protein

The digested DNA inserts were isolated from 1% agarose gels and ligated into the NheI/NotI cut and dephosphorylated mammalian episomal expression vector pCEP-Pu (Kohfeldt *et al.*, 1997)(kindly provided by Prof. Dr. Mats Paulsson, University of Cologne, Cologne, Germany). pCEP-Pu contains a puromycin resistance for convenient cell selection, as well as a His₆-Myc tag followed by a Factor-X cleavage site just

2. Materials and Methods

preceding the multiple cloning site. HEK293/EBNA cells (Invitrogen, Carlsbad, CA) were electroporated with the constructs and stable transfection achieved by selection with puromycin (see 2.3.4). The protein expression was carried out like described in 2.3.5. The fusion proteins were purified by affinity chromatography on a cobalt column (Talon™, BD Biosciences, Palo Alto, CA) as described in the manufacturer's instructions:

For purification, 200 ml of the tagged proteins was thawed and dialyzed over night against His-1-buffer (50 mM NaH₂PO₄, 20 mM Tris, 100 mM NaCl, pH 8). The solution was applied to the His-1-buffer equilibrated column at a flow rate of 1 ml/min. After all solution was applied the column, the column was washed with 15 ml His-1-buffer. To eliminate unspecific background binding, the column was washed with 5 bed volumes of His-2-buffer (His-1-buffer + 10 mM Imidazol). Bound protein was eluted with 3 times 5 ml of His-3-buffer (His-1-buffer + 250 mM Imidazol). Fractions containing pure protein were identified by SDS-PAGE, pooled and dialyzed against 1/10 PBS. The dialyzed samples were concentrated 10 times by using the Ultrafree®-15 Centrifuge Filter Device (Millipore, Billerica, MA), checked for purity by SDS-PAGE and stored in aliquots at –80°C.

The column was regenerated by stripping the column with 10 bed volumes of 20 mM MES-buffer (2-(N-morpholine)-ethanesulfonicacid). Next, the column was rinsed with 5 bed volumes of dd-H₂O and equilibrated with His-1-buffer. Columns were then reused or stored in 20% Ethanol containing 0.1% sodiumazide at 4°C.

2.2.4 Solid phase binding assay

All of the following steps were performed at room temperature. Laminin-1 was diluted to 10 µg/ml with 50 mM sodium bicarbonate pH 9.6 (coupling buffer) and immobilized on 96-well plates (100 µl/well; Maxisorb plates, Nunc, Roskilde, Denmark and Falcon regular 96-well plates) by incubation over night. To prevent nonspecific interactions, remaining binding sites were saturated by incubation with 5% dry milkpowder in TBS (400 µl/well) for 2 hours. After blocking, the wells were incubated for 2 hours with the recombinant proteins at different concentrations (1 nM - 100 nM) in TBS containing 0.03 mg/ml κ-casein (Sigma, St. Louis, MO). As a control, laminin-1 coated wells were

2. Materials and Methods

incubated with casein at the same concentrations (1 mM – 100 mM). Next, the wells were washed 3 times with TBS containing 0.05% Tween-20. To detect bound antigen, a monoclonal antibody against the fused myc-tag was used (mouse monoclonal IgG antibody (c-Myc (9E10): sc-40; Santa Cruz Biotechnology, Santa Cruz, CA; Dilution: 1:2500 in TBS containing 0.03 mg/ml κ -casein; 100 μ l per well; incubation: 1 hour). The wells were washed 3 times with TBS containing 0.05% Tween-20 (100 μ l/well), followed by incubation with secondary peroxidase-conjugated antibody (Peroxidase goat-anti mouse; Dilution 1:2500) in TBS containing 0.03 mg/ml κ -casein for 1 h. Finally, the wells were washed 3 times with TBS containing 0.05% Tween-20 (100 μ l/well) and three times with water (100 μ l/well). The enzyme reaction was started with 3,3',5,5'-Tetramethylbenzidine (TMB) Liquid Substrate for ELISA (Sigma; 100 μ l/well), which in the presence of peroxidase produced a pale blue soluble product. This reaction was stopped by adding 20% H₂SO₄ (100 μ l/well) which converted the solution to yellow in color. Extinction was then measured at 450 nm using a spectrophotometer. The extinction values were plotted against the protein concentration in nM and the EC₅₀-value was determined by using the OriginTM-software using a sigmoidal fit.

2.2.5 N-Glycanase treatment

100 μ g protein was diluted in 20 mM sodium phosphate pH 7.5, containing 0.02% sodium azide. The protein was then denatured at 100°C for 5 minutes in the presence of 0.1% SDS, and 50 mM β -mercaptoethanol. After cooling, NP-40 was added to a final concentration of 0.75% and 5 mU N-Glycanase (Glyko, Inc.) was added to the reaction mixture and incubated for 2 hours to overnight at 37°C.

2.2.6 Chondroitinase ABC digestion

To remove chondroitin sulfate chains from recombinant proteins, the samples were dialyzed against PBS pH 8.0 and treated with chondroitinase ABC (Seikagaku, Rockville, MA) (1-2 milliunits/ μ g of proteoglycan).

To minimize the risk of core protein self-aggregation upon glycosaminoglycan chain removal, the reaction was stopped after 2 hours at 37°C by adding SDS-sample buffer and boiling the samples for 5 minutes. Samples were run on a 10%- or a 3.5-15% linear gradient SDS-PAGE gel and transferred to a nitrocellulose membrane. Proteins were then detected using a monoclonal antibody against the fused myc-tag.

2.2.7 Heparitinase digestion

To remove heparansulfate chains from recombinant proteins, the samples were dialyzed against PBS pH 7.0 containing 3 mM CaCl₂ and treated with heparitinase (Sigma, St. Louis, MO) (0.125 milliunits/ μ l).

To minimize the risk of core protein self-aggregation upon glycosaminoglycan chain removal, the reaction was stopped after 2 hours at 37°C by adding SDS-sample buffer and boiling the samples for 5 minutes. Samples were run on a 10%- or a 3.5-15% linear gradient SDS-PAGE gel and transferred to a nitrocellulose membrane. The protein was detected using a monoclonal antibody against the fused myc-tag.

2.2.8 Limited tryptic digestion

Protein samples (5-20 μ M) were incubated with 5U trypsin/ μ mol of protein at room temperature in 50 mM Tris-HCl containing 200 mM NaCl. The reaction was stopped after one hour by adding SDS-sample buffer and boiling the samples for 5 minutes at 95°C. The proteins were analyzed by SDS-PAGE and visualized by silver staining.

2.3 Cell Culture

The equipment used in cell culture was either autoclaved glassware or sterile packed plastic equipment. The used solutions were either autoclaved, sterile filtered or obtained as sterile solutions. Cells were cultured at 37°C in a water-saturated atmosphere with a CO₂-content of 5%. All work was performed in a sterile-hood.

2.3.1 Cells

HEK293/EBNA cells (Invitrogen, Carlsbad, CA) were cultured in DMEM supplemented with 10% fetal calf serum (Gibco Life Technologies Inc., Rockville, MA), 1% L-glutamine, penicillin, streptomycin and 350 µg/ml Geneticin (G418, Gibco, stock: 50 mg/ml,) at 37°C in a 5% CO₂ atmosphere. Medium was changed every other day and the cells were passaged every 4-5 days.

2.3.2 Trypsinization

Medium was discarded and the cells washed with 1x PBS. 2 ml trypsin was added and the cells incubated at 37°C. The cells were spun down, resuspended in EBNA-medium and distributed to new plates.

2.3.3 Transfection

The cells were washed 3 times with TBS, trypsinized, centrifuged and resuspended in EBNA-medium. Cell density was measured with a hemacytometer (Fisher Scientific, Pittsburgh, PA).

2.5×10^5 cells in 500 µl Medium were incubated with 4–5 µg of DNA for 5 minutes. Electroporation was performed at 220 Volts, with a single 10 ms pulse using the ElectroSquarePorator™ ECM 830 (BTX/Genetronics, San Diego, CA).

2. Materials and Methods

2.3.4 Selection

Transfectants were grown in EBNA-medium for 2 days and then selected by adding 1 µg/ml puromycin to the medium. Selection was carried on for 14-18 days in DMEM, 10% FCS, 100x L-glutamine (200mM), 100x penicillin/streptomycin, 1 µg/ml puromycin (stock: 5 mg/ml)

2.3.5 Protein expression

Cells were then grown to confluency, washed three times with TBS, then 20 ml serum free medium (DMEM/F12-Nutrient Mix 1:1, 100x L-glutamine (200 mM), 100x penicillin/streptomycin, 1 µg/ml puromycin (stock: 5 mg/ml)) was added per 150 mm by 25 mm dish (“Integrid”; Falcon 353025). Supernatant was collected every other day for 10 days, spun down to remove dead cells (which over time could release proteases into the solution and thus degrade the desired proteins), and stored at -20°C until purification.

2.3.6 Neurite outgrowth assays

Tissue culture dishes were coated with nitrocellulose, dissolved in methanol as described (Lagenaur and Lemmon, 1987). 3 µl of the various agrin peptides at the concentration of ~360 nM were applied as a small stripe on a dish. After 5 minutes of incubation, the coated stripe was washed twice with PBS. The stripe plus the adjacent nitrocellulose area were then coated with 10 µl of 20 µg/ml laminin. After 5 minutes of incubation the coated area was washed with DMEM/5% FCS.

Dorsal root ganglia were dissected from E8 chick embryos and transferred onto the coated dishes. To promote the adhesion of the ganglia, the medium was removed and the ganglia incubated on the moist substrate for 1 hour. Finally 100 µl of DMEM with 5 ng/ml NGF was carefully added to the cultures. After 30 hours of incubation, 1 µl of the anti-myc-antibody was added to the cultures, followed by fixation 1 hour later with 4% para-formaldehyde (PFA). The cultures were stained with a monoclonal antibody (MAb) to tubulin (MAb 6G7) followed by alkaline-phosphatase labeled goat anti-mouse secondary antibody. Myc-labeled substrate and axons were visualized with BCIP/NBT.

2.4 Histology

Heads of chick embryos were fixed in 4% paraformaldehyde in 0.1M potassium phosphate buffer (pH 7.4) for 1 h. After washing in CMF and cryoprotecting with 30% sucrose for 4 h, the specimens were embedded in O.C.T. compound (Miles, Elkhart, IN) and sectioned in a horizontal plane with a cryostat at 25 μ m. Sections were mounted on Superfrost slides (Fisher Scientific, Pittsburgh, PA). The sections were permeabilized with 0.05% Triton X-100 and 1% BSA for 10 min and incubated with the first antibody for 1 h. After three rinses, the sections were incubated with 1:500 Cy3-labeled goat-anti mouse or goat-anti rabbit antibodies (Jackson ImmunoResearch, West Grove, PA) for another hour. After two final rinses, the specimens were mounted in 90% glycerol and examined with an epifluorescence microscope (Zeiss, Thornwood, NY) or a confocal microscope (Fluoview; Olympus, Lake Success, NY).

2.4.1 Disruption and regeneration of the retinal basal lamina

For basal lamina regeneration experiments, 0.5–1 ml of 100 U/ml (~70 mg/ml) collagenase (Sigma, St. Louis, MO) was injected into E3–E5 eyes (Halfter, 1998), and the collagenase was chased with 1 ml of laminin-1 (Gibco/BRL) at 1 mg/ml. The embryos were sacrificed 24 h after the laminin-1 chase, and sections through the heads were stained with chick specific antibodies to laminin-1 and agrin to determine the presence of an intact retinal basal lamina.

2.5 Equipment

Electrophoresis Equipment:

- Amplifier: Techware PS 500-1, Sigma Aldrich, St. Louis, MO, USA
- Vertical: SE 260 Mighty Small, Hoefer Scientific Instruments, San Francisco, CA, USA
- Horizontal: HE 33 Mini Horizontal, Hoefer Scientific Instruments, San Francisco, CA, USA
- Electrotransfer: Trans-Blot® SD, Semi-Dry Transfer Cell, BioRad, Hercules, CA, USA

Electroporation: ElectroSquarePorator® ECM 830, BTX/Genetronics, San Diego, CA, USA

Shaker: Red Rocker, Hoefer Scientific Instruments, San Francisco, CA, USA

Peristaltic Pump: Econopump, BioRad, Hercules, CA, USA

pH-Meter: Digital Ionalyzer/501, Orion Research, Beverly, MA, USA

Photometer: GeneQuantII RNA/DNA Calculator, Pharmacia Biotech, Cambridge, UK

PCR:

- PCR-Sprint: HyBaid, Teddington, Middlesex, UK
- Mastercycler Gradient: Eppendorf-Netheler-Hinz GmbH, Hamburg, Germany

Centrifuges:

- Eppendorf 5415C: Eppendorf-Netheler-Hinz GmbH, Hamburg, Germany
- Beckmann CS-6: Beckmann Instruments Inc., Fullerton, CA, USA

Scales:

PM300 Mettler-Toledo AG, Greifensee, Germany

R 160 D Sartorius Research, D-37075 Goettingen, Germany

Transluminator: TW-26, VWR, NJ,

Microscope: TMS, Nikon, Japan

2.6 Solutions, buffers, and media

10x SDS-Sample buffer

0.1 M Tris (1.21 g in 50 ml, pH to 6.8)

10% SDS (add 10 g, bring to 70 ml)

10 ml of Bromphenolblue (from 0.4% Stock)

20 ml Glycerol

for reducing conditions, add 50 μ l β -mercaptoethanol per ml sample buffer

SDS-electrophoresis buffer

25 mM Tris

192 mM Glycine

0.1% SDS

Transfer buffer

25 mM Tris

192 mM Glycine

0.01% SDS

1xCMF-PBS

8 g NaCl

0.2 g KCl

1.15 g Na₂HPO₄

0.2 g KH₂PO₄

2. Materials and Methods

Alkaline phosphatase developing buffer:

0.1 M Tris
0.1 M NaCl
0.05 M MgCl₂

1x TBS

50 mM Tris
150 mM NaCl
→ adjust pH to 7

TAE-Buffer (50x)

242 g Tris Base
57.1 ml glacial acetic acid
37.2 g Na₂EDTAx2H₂O
→ add H₂O to 1 Liter ≈ pH 8.5
⇒ 1x working solution
40 mM Tris acetate
2 mM EDTA

TE

10 mM Tris/HCl pH 7.4
1 mM EDTA pH 8

LB-Medium

21 g NZY-Broth
→ add 1 liter dd-H₂O
→ autoclave

Bacterial plates:

25 g LB + 15 g Bacto-Agar
ad 1 L with water

autoclave

Tetracycline: Stock: 12.5 mg/ml⇒EK 12.5 µg/ml

Ampicillin: Stock: 100 mg/ml⇒EK 100 µg/ml

Coomassie Blue

0.5% Coomassie/MeOH

2.5 g Coomassie + 497.5 g MeOH

→ stir over night

→ filter

→ before usage mix 1:1 with 20% HAc

2.7 Antibodies

2.7.1 Primary antibodies

Rabbit anti-NGF 2.5 S (Sigma, St. Louis, MO)

Mouse monoclonal IgG antibody (c-Myc (9E10): sc-40; Santa Cruz Biotechnology, Santa Cruz, CA)

Mouse monoclonal antibody to chick laminin (3H11, provided by Prof. Willi Halfter, Univ. of Pittsburgh)

Mouse monoclonal antibody to tubulin (6G7, provided by Prof. Willi Halfter, Univ. of Pittsburgh)

2.7.2 Secondary antibodies

Cy3-labeled goat-anti mouse or goat-anti rabbit antibodies (Jackson ImmunoResearch, West Grove, PA)

Peroxidase conjugated goat-anti mouse (Jackson ImmunoResearch, West Grove, PA)

Alkaline phosphatase conjugated goat-anti mouse (Jackson ImmunoResearch, West Grove, PA)

Alkaline phosphatase conjugated goat-anti rabbit (Jackson ImmunoResearch, West Grove, PA)

3. Results

In order to investigate the properties of the N-terminal domains of agrin, 9 different fragments and a total of approximately 30 mutants were investigated.

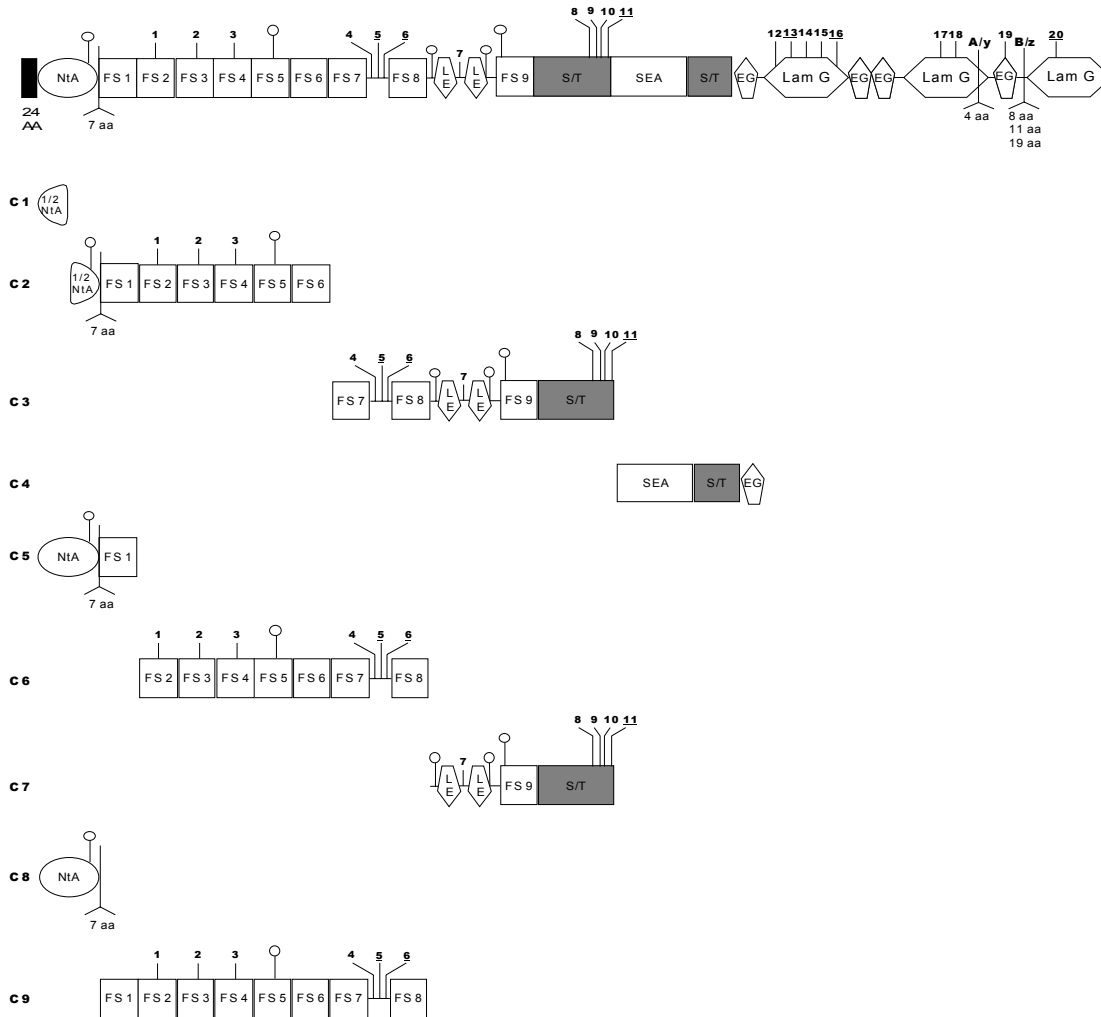


Figure 9 Schematic diagram depicting the domain structure of the agrin core protein. The fragments (PF1 to PF9) that were expressed for the present study are listed below. The SGs as potential attachment sites for GAGs are numbered from 1 to 20; the SGs within a more defined SGXG consensus sequences are underlined. Abbreviations for the domains: NtA: N-terminal agrin domain, FS: follistatin-like domains; LE: laminin EGF-like module; S/T: serine/threonine-rich domain; SEA: module first found in sea urchin sperm protein; EG: EGF-like repeat; Lam G (LG): laminin G-like domains. The three splice sites of agrin are also indicated. The domain borders were assigned based on results from the ProDom-NCBI-BlastP 2.0.8 World Wide Web server in may of 2000 (www.prodes.toulouse.inra.fr/cgi-bin/). In the meantime, there is a newer version of this software (BlastP 2.2.1) which gives rise to slightly different assignments, which have no impact on this study.

3. Results

Table 1 Overview over the protein fragments expressed and investigated in this study.

Fragment	comprising AA ^a	comprising domains	Mw [kDa] ^b
PF1	AA 1-94	1/2 NtA	15.8
PF2	AA 95-616	1.-7. FS domain	61.9
PF3	AA 594-1116	7.FS-beginning SEA domain including 2 pot. multiple GAG attachment sites	60.2
PF4	AA 1117-1376	SEA domain-beginning LamG	33.7
PF5	AA 1-229	NtA + 1.FS	30.8
PF6	AA 223-744	2. FS - 8.FS including 1. pot multiple GAG attachment site	61.7
PF7	AA 738-1116	LE domain-beginning SEA including 2. pot. multiple GAG attachment site	44.5
PF8	AA 1-172	NtA	24.7
PF9	AA 169-744	1.FS - 8. FS including 1. pot. GAG attachment site	67.5

^a Comprising amino acids starting from Asn 25 of chick agrin (U 35613), consistent with the first amino acid after the proposed signal sequence cleavage site (Denzer et al, 1997).

^b Theoretical molecular weights of the proteins as determined by using the ProtParamTool World Wide Web Server (<http://us.expasy.org/tools/protparam.html>)

All proteins were expressed in a eucaryotic expression system utilizing HEK293/EBNA cells. The recombinant proteins were purified over a cobalt-based column utilizing the fused His₆-tag. The purity of all fragments was checked by SDS-PAGE.

3. Results

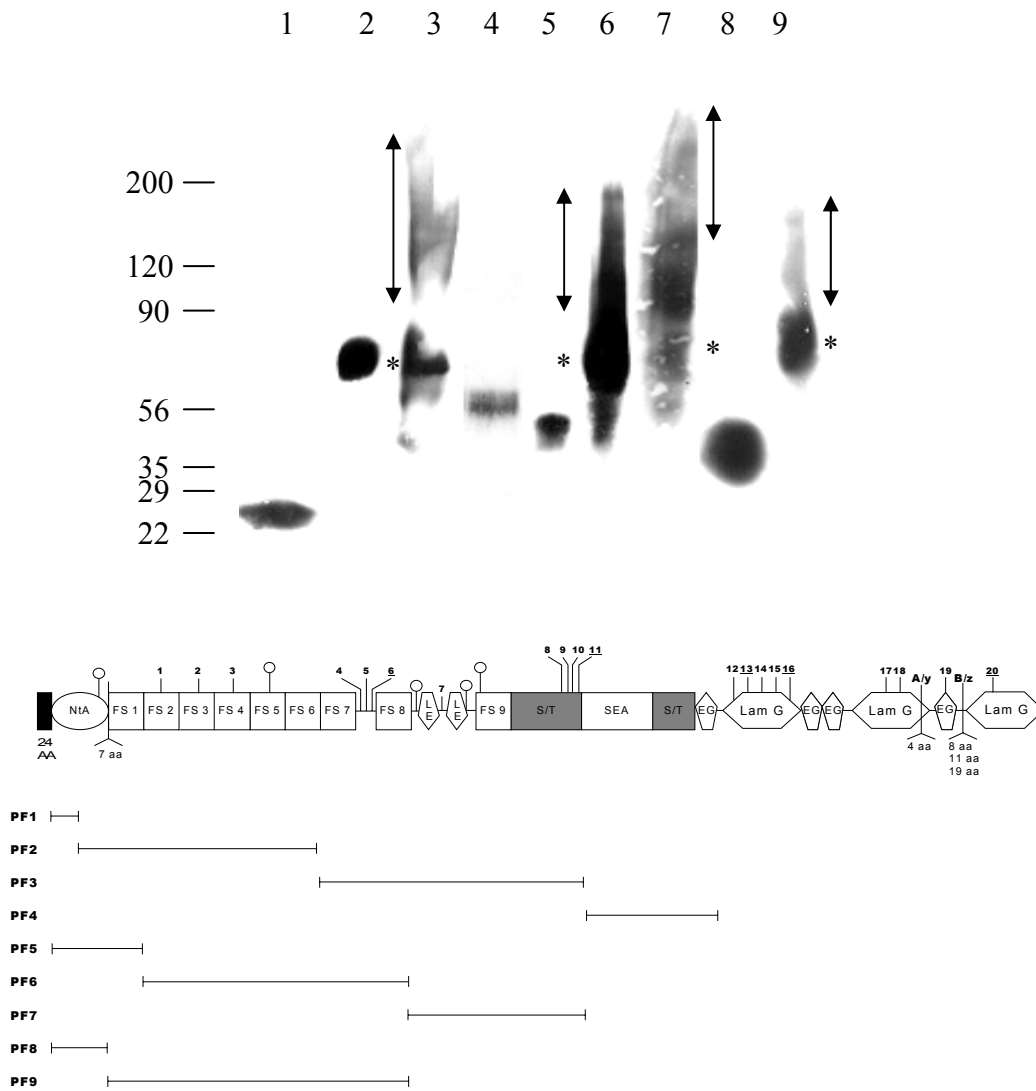


Figure 10 Western blot showing the various agrin fragments after separation by SDS-PAGE. The diagram of agrin and the expressed agrin fragments are listed below. Four of the fragments: PF3, PF6, PF7 and PF9 show long trails of immunoreactivity typical for peptides connected to GAGs. The stars indicate the core proteins; double-headed arrows indicate the size range of the glycosylated peptides. All other fragments (PF1, PF2, PF4, PF5 and PF8) appear as defined bands indicating that these peptides are not GAG glycosylated.

3. Results

Discrepancies between apparent masses and calculated masses can be explained with multiple N-glycosylation sites within the agrin protein. There are 5 consensus sequences for N-glycosylation in agrin. In other proteins, these N-X-S/T “sequons” were shown to carry sugars in 90% of the investigated cases (Bause, 1983; Gavel and von Heijne, 1990; Imperiali and Rickert, 1995).

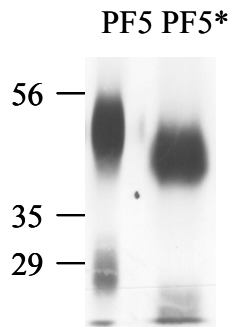


Figure 11 Western blot of N-glycanase treatment of PF5.

3.1 Binding to laminin-1

Previous studies utilizing 1. full-length agrin, 2. an agrin fragment comprising the NtA and the 1. FS-domain (NtA-FS) and 3. a full length agrin fragment that lacks the first 130 amino acids from the N-terminus (cΔN agrin) were able to pinpoint the laminin-binding site to the very N-terminal domain of agrin (NtA) (Denzer *et al.*, 1997; Denzer *et al.*, 1995; Denzer *et al.*, 1998). Because the NtA-domain containing fragment used in the former studies was fused to the 1. FS domain, it was actually never shown that the NtA-domain alone is sufficient for laminin binding. In accordance with the results obtained from ProDom-NCBI-BlastP 2.0.8, a fragment consisting of the amino acids upstream from the first FS-domain (amino acids 1-172) was expressed in HEK293/EBNA cells. Furthermore a fragment comprising the N-terminal half of the NtA-domain (amino acids 1-94; PF1), a fragment containing the C-terminal half of the NtA (amino acids 95-616; PF2), and the previously described NtA-FS fragment (amino acids 1-229; PF5) were expressed and purified utilizing the fused His₆-tag. The purity of the used proteins was checked on SDS-PAGE.

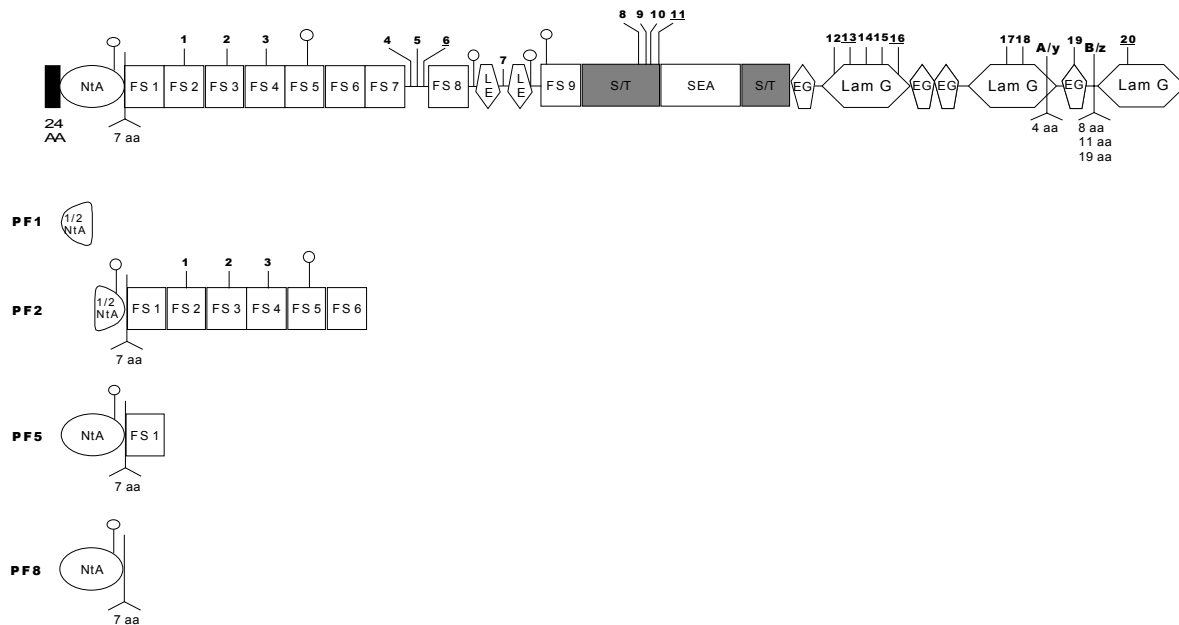


Figure 12 Protein fragments used for investigating the laminin-binding property of agrin

3. Results

The binding affinity to laminin-1 was determined using a solid phase binding assay. Laminin-1 was coated to a 96-well plate and incubated with the different fragments in a concentration gradient. A color reaction of the peroxidase-conjugated secondary antibody with ready-to-use TMB-liquid was used to quantify the binding of the various fragments to laminin. The reaction was stopped with H_2SO_4 resulting into a yellow solution and its extinction was measured at 450 nm with an ELISA-reader.

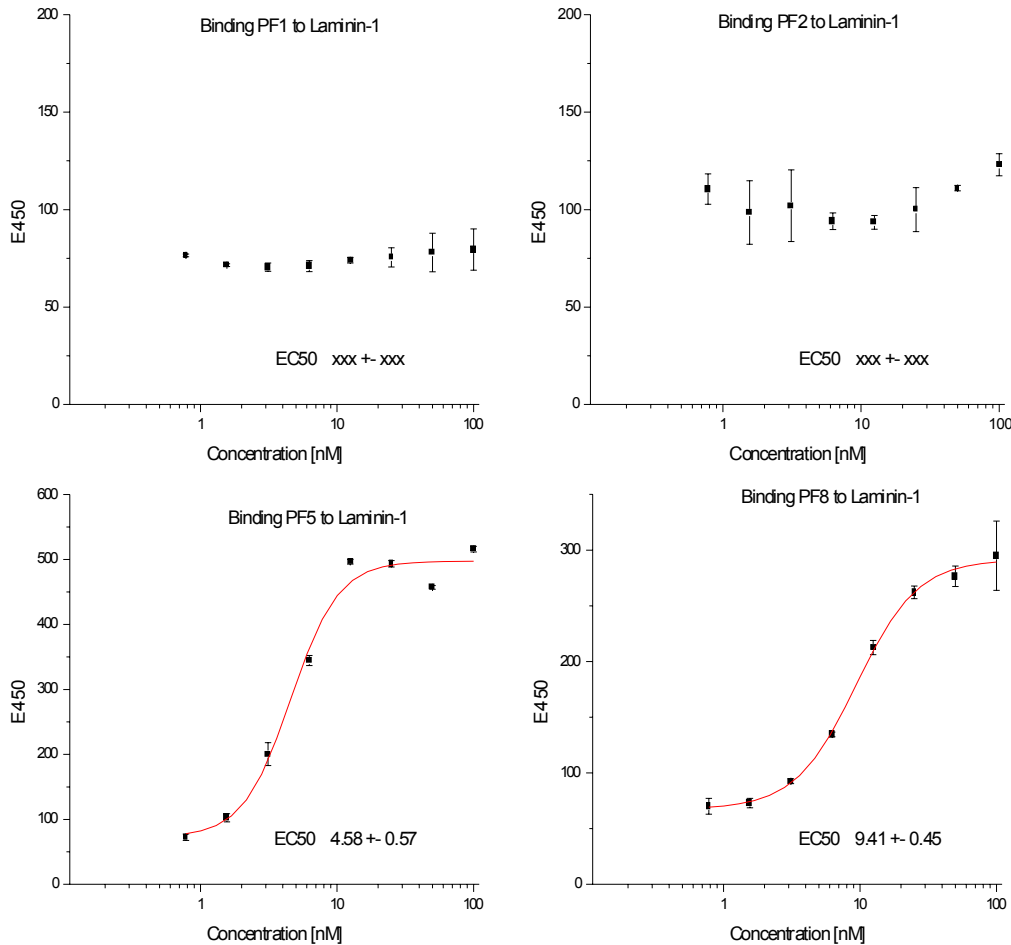


Figure 13 Dose-response curve of the binding of different agrin constructs to laminin-1. The binding curves shown are results of one representative experiment with the corresponding background (laminin-1 coated wells incubated with κ -casein) subtracted. Half-maximal binding was determined using the OriginTM-software and using the sigmoidal fitting option. Values shown are the mean +/- SD from two measurements. All experiments were repeated at least 4 times. Note that EC_{50} values varied up to 100% between independent measurements.

3. Results

Table 2 Different protein fragments containing the NtA-domain or parts of this domain and their affinity to laminin-1

Fragment	comprising AA	Half maximal binding ^a	Relative Binding ^b
PF5	AA 1-229 (NtA-FS)	5	1
PF8	AA 1-172 (NtA)	10	2
PF1	AA 1-94	no binding	no binding
PF2	AA 95-616	no binding	no binding

^a the concentration (nM) required to achieve half maximal binding determined by ELISA

^b relative binding refers to the ratio of half maximal binding of mutant/NtA-FS

Because EC₅₀ values varied up to 100% between independent measurements each peptide was measured at least 4 times. The values depicted in the tables are the mean value of the obtained results. On immobilized laminin-1, PF5 reached half-maximal binding (EC₅₀) at ~5 nM (Figure 13) consistent with previous studies that have shown a strong binding of full-length agrin to laminin-1 with a EC₅₀ of ~5 nM (Denzer *et al.*, 1997). This indicates that the additional His₆-Myc-Tag does not interfere with the binding property of the recombinant protein. The work of Mascarenhas *et al.* showed that the results obtained in this assay matched the results obtained in a competition assay with ¹²⁵I labeled NtA-FS protein (Mascarenhas *et al.*, 2003).

The data show similar binding activities for both NtA (EC₅₀ ~10 nM) and NtA-FS (EC₅₀ ~5 nM) while no binding activity was detected for PF1 and PF2, indicating that the binding activity of agrin is located in the NtA alone (Figure 13). Furthermore, parts of this domain are not sufficient for this property suggesting that the 3-dimensional structure of the domain has to remain intact for the laminin-binding to occur.

To verify the laminin-binding results *in vivo*, fragments PF1 and PF8 were injected into embryonic day 8 (E8) chick embryos vitreous body at a concentration of 0.3 mg/ml. After the fragment PF8 remained in the vitreous for 24 hours, the retinal basal lamina as well as the basal lamina of the lens showed anti-myc staining (Figure 14), while no staining was detectable for PF1 (data not shown). This indicates that fragment PF8 bound to the laminin present in the basal lamina.

Furthermore an experiment was conducted in which the basal lamina was dissolved by injection of collagenase into the vitreous of embryonic chick eyes. Its regeneration was induced by a chase with mouse laminin-1. The regeneration occurred within 6 h after the

3. Results

laminin-1 chase by forming a morphologically complete basal lamina that included all known basal lamina proteins from chick embryos, such as laminin-1, nidogen-1, collagens IV and XVIII, perlecan, and agrin (Halfter *et al.*, 2001). In the present study laminin-1 (final concentration: 1 mg/ml) was pre-incubated for 1 hour with 0.15 mg/ml (final concentration) of either PF1 or PF8.

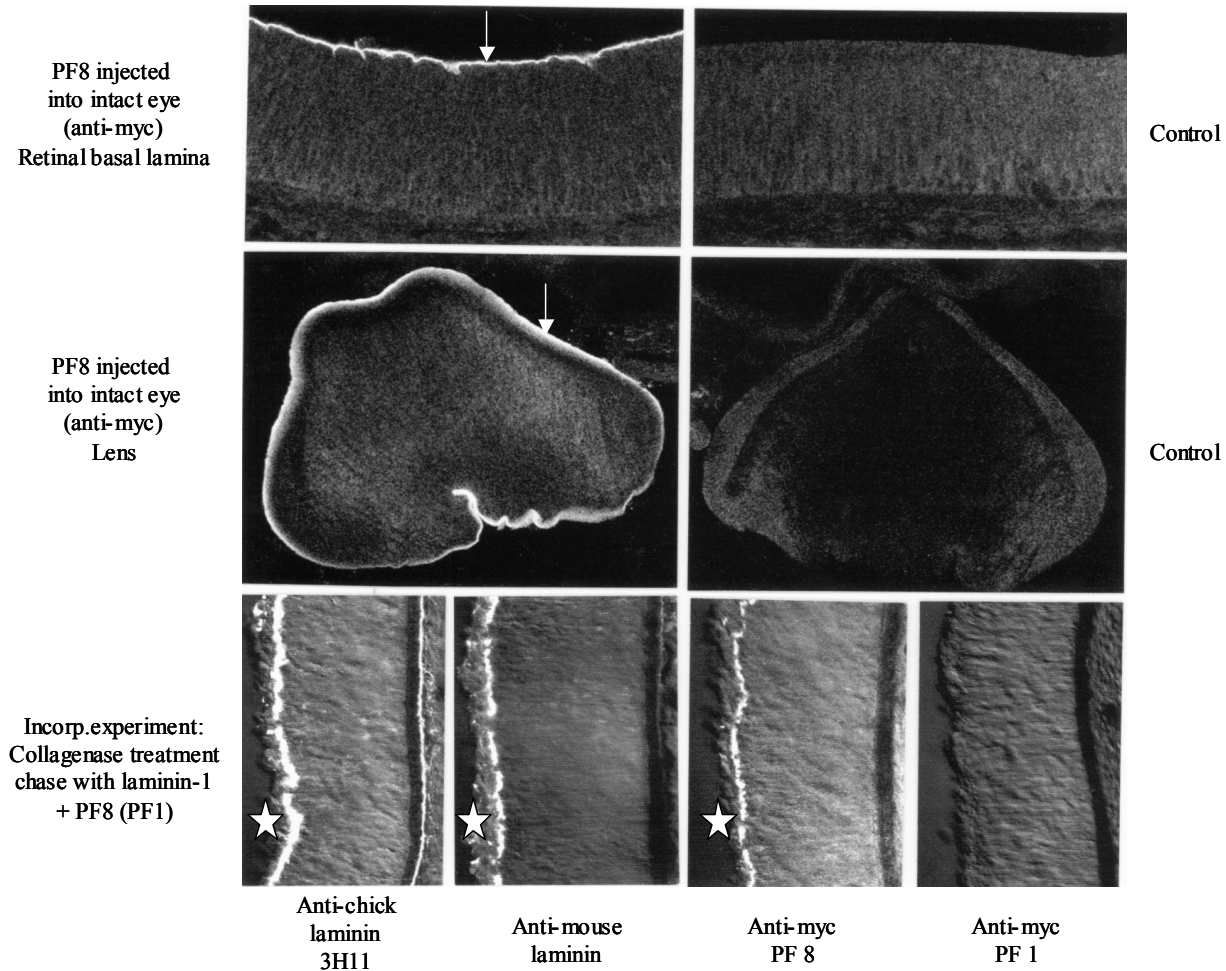


Figure 14 Upper left: PF8 injected into intact eye (anti-myc staining) retinal basal lamina, upper right: control untreated eye, middle left: PF8 injected into intact eye (anti-myc staining) Lens, middle right; control untreated eye, bottom row from the left: laminin-chase experiment, the eye was injected with collagenase at E4, and chased 10 hours later with mouse laminin-1 plus PF8 or PF1; laminin-1 (conc: 2mg/ml, mixed 1:1 with the peptide). The embryo was sacrificed 24 hours later. Staining with MAb 3H11 to chick laminin (Halfter, 1993) and staining with a polyclonal antiserum to mouse laminin-1 shows that the injected mouse laminin-1 caused the reconstitution of the chick retinal basal lamina. Staining with a MAb to c-myc shows that PF8 but not PF1 got incorporated into the newly formed basal lamina.

The newly generated retinal basal lamina showed anti-myc staining co-localized with staining against mouse laminin-1 in the case of PF8 but not for PF1, indicating that PF8 bound to mouse laminin-1 during the pre-incubation process and the complex of laminin-1 and PF8 got

3. Results

incorporated into the newly formed basal lamina (Figure 14). All these experiments prove that the NtA (PF8) is the critical domain for agrin's laminin-binding activity. These *in vivo* results are consistent with *in vitro* findings established by the solid phase binding.

To investigate the laminin-binding site in more detail, PF5 (NtA-1.FS) was used as template for site-directed mutagenesis experiments. Because previous experiments in this thesis revealed that the NtA alone is the crucial domain for laminin binding, mutations were only performed within the NtA-domain. To determine the amino acids necessary for the binding mechanism, highly conserved positively charged amino acids (R and K) that were conserved in the NtA-domains of agrin's from different species, were chosen for site-directed mutagenesis.

The deduced amino acid sequences of mouse, chick, and human NtA are highly homologous to each other. The homology starts at residue 26 of chick agrin, which corresponds to the predicted cleavage site for the signal sequence (Denzer, 1995). From AA 26 to 149, 96% of the amino acids are identical between mouse and human and 90% are identical between chick and the mammalian sequences.

```
chick  NCPERELQRREEEEANVVLGTGTVVEEIMNVDPVHHTYSCKVRVVWRYLKGKDIVTHEILLDGGNKVV
human  TCPERALERREEEEANVVLGTGTVVEEILNVDPVQHTYSCKVRVVWRYLKGKDLVARESLLDGGNKVV
mouse  TCPERALERREEEEANVVLGTGTVVEEILNVDPVQHTYSCKVRVVWRYLKGKDVVAQESLLDGGNKVV

chick  IGGFGDPLICDNQVSTGDTRIFFVNPAPQYMWPAHRNELMLNSSLMRITLRNLEEVEHCVEEHR
human  ISGFGDPLICDNQVSTGDTRIFFVNPAPPYLWPAHKNELMLNSSLMRITLRNLEEVEFCVE---
mouse  IGGFGDPLICDNQVSTGDTRIFFVNPAPPYLWPAHKNELMLNSSLMRITLRNLEEVEFCVE---

chick  KLLADKPNSYFTQTPPTPRDAC
human  ----DKPGTHFTVPPTPPDAC
mouse  ----DKPGIHFTAAPSMPPDVC
```

Figure 15 Alignment of the laminin-binding domain of chick, human and mouse. The sequences were aligned to the first 150 amino acids of chick agrin starting after the proposed signal sequence cleavage site (Denzer *et al.*, 1997). Amino acids between Cys 2 and Glu 125 are almost 90% identical between the examined species. Highly conserved, positively charged amino acids (R and K) were depicted in bold/red letters. Bold/blue letters indicate substitutions of similar amino acids. The sequences were derived from the GenBank/EMBL/DDBJ with the following accession numbers: U35613 (chick), U 84406 (human) and U84407 (mouse). Underlined amino acids depict potential N-glycosylation sites

In total, 8 mutants were investigated in the laminin-binding study and various other mutants were investigated by another research group working on the same subject. All mutated proteins were obtained from serum-free culture medium of transfected HEK293/EBNA cells and purified using the His₆-tag over a cobalt-based column. The purity of all mutant proteins was checked by SDS-PAGE and proper folding was tested performing a limited tryptic digest.

3. Results

All the examined proteins showed resistance to treatment with trypsin (data not shown) indicating proper folding of the peptides. The binding affinity of the different mutants to laminin-1 was determined using a solid phase binding assay.

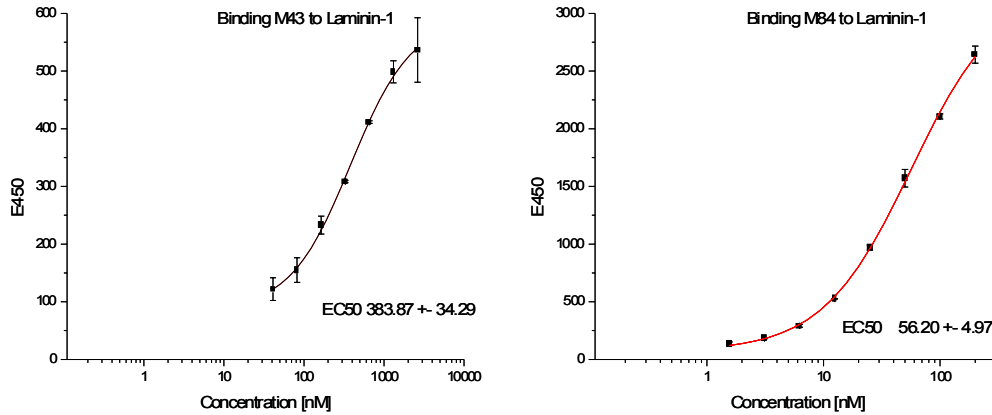


Figure 16 Dose-response curve of the binding of different PF5 mutants to laminin-1. The binding curves shown are results of one representative experiment with the corresponding background (laminin-1 coated wells incubated with κ -casein) subtracted. Half-maximal binding was determined using the Origin™-software and using the sigmoidal fitting option. Values shown are the mean \pm SD from two measurements. All experiments were repeated at least 4 times. Note that EC_{50} values varied up to 100% between independent measurements.

Table 3 Effect of mutations of the NtA-FS domain on its laminin-1 binding activity

Mutant	AA effected	Half maximal binding ^a	Relative Binding ^b
M5	R5A	8	1.6
M9,10	RR9,10AA	24	4.8
M5,9,10	RRR5,9,10AAA	63	12.6
M43	R43A	380	76
M84	R84A	56	11.2
M111	R111A	-	-
M115	R115A	23	4.6
M128,129	RK128,129AA	11	2.2

^a the concentration (nM) required to achieve half maximal binding determined by ELISA

^b relative binding refers to the ratio of half maximal binding of mutant/NtA-FS

Of all point mutations, only replacement of R43 and R111 showed notable effects. While the mutation of R43 led to a 80-fold decrease in the binding affinity towards laminin-1, mutation of R111 led to an extreme decrease in the protein expression rate of the protein, which could indicate that the expressed protein is not stable. This fragment also did not show any binding in the solid phase binding assay. To analyze a possible influence of the splice insert on the

3. Results

binding affinity, the two positively charged amino acids R128 and K129 were changed to alanines. These mutations showed no effect on the laminin-binding property of the NtA-FS fragment. These results are consistent with the finding that a mutant protein lacking the splice insert (Δ splice) showed the same affinity to laminin-1 as the fragment containing the 7-residue insert (Mascarenhas *et al.*, 2003). Also, single mutations in the most N-terminal α -helix (helix 1; R5, R9, R10) did not show any major effect on the laminin-binding ability of the NtA. This is consistent with a previous publication in which a deletion of the N-terminal helix did not alter the laminin-binding affinity of agrin (Stetefeld *et al.*, 2001).

Additional studies have shown that the N-glycosylation within the NtA-domain is not essential for this effect (Mascarenhas *et al.*, 2003).

3.2 Fusion protein with NGF

In an approach to create a fusion protein that would exhibit both, binding to laminin and growth factor properties, PF5 as well as PF8 were fused to the biological active form of mouse-NGF, giving rise to peptides N5 and N8. The fusion proteins were expressed with an N-terminal His₆-Myc-tag, which allowed easy purification over a cobalt-based column and easy detection with an anti-myc monoclonal antibody.

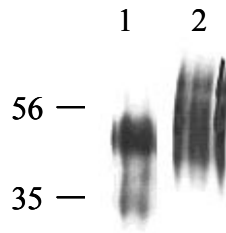


Figure 17 Western blot of PF5 fused to NGF-mature (N5) using the anti-myc monoclonal antibody (lane 1) and using a polyclonal anti-NGF antibody (Rabbit anti-NGF 2.5 S, Sigma, St. Louis, MO; lane 2).

To evaluate whether the fused NGF interfered with the laminin-binding ability of these two fragments, a solid phase binding assay was performed. The experiments were conducted under the same conditions as the experiments in chapter 3.1 to allow comparison of the resulting EC₅₀-values.

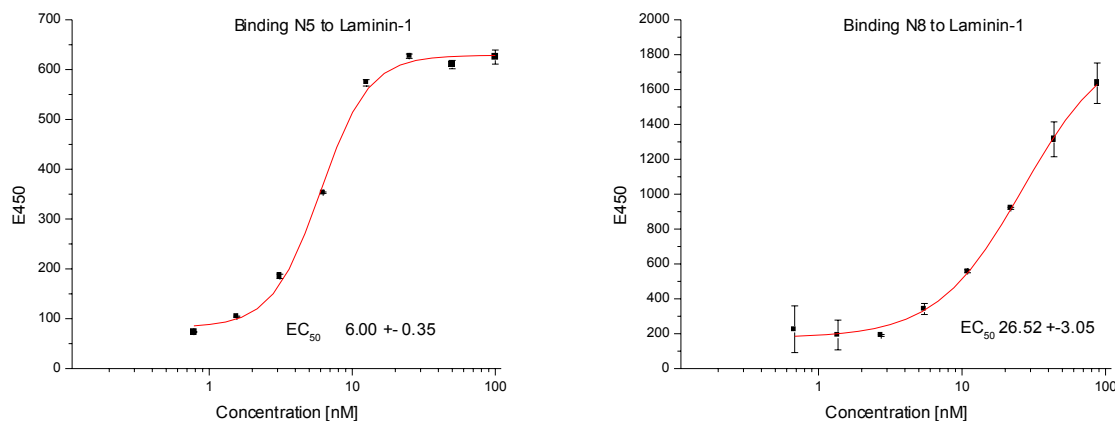


Figure 18 Dose-response curve of the binding of NGF-fused agrin peptides to laminin-1. The binding curves shown are results of one representative experiment with the corresponding background (laminin-1 coated wells incubated with κ -casein) subtracted. Half-maximal binding was determined using the Origin™-software and using the sigmoidal fitting option. Values shown are the mean ± SD from two measurements. All experiments were repeated at least 4 times. Note that EC₅₀ values varied up to 100% between independent measurements

3. Results

While in the case of N5, NGF does not seem to interfere with the laminin-binding property of the peptide (Figure 18), N8 ($EC_{50} \sim 25$ nM) exhibits a slight decrease in laminin-binding activity compared to the unfused protein PF8 ($EC_{50} \sim 10$ nM) (Figure 18 and Figure 13).

To verify the results obtained in the solid-phase binding assay, N8 was subject to collagenase/laminin-chase experiments *in vivo*.

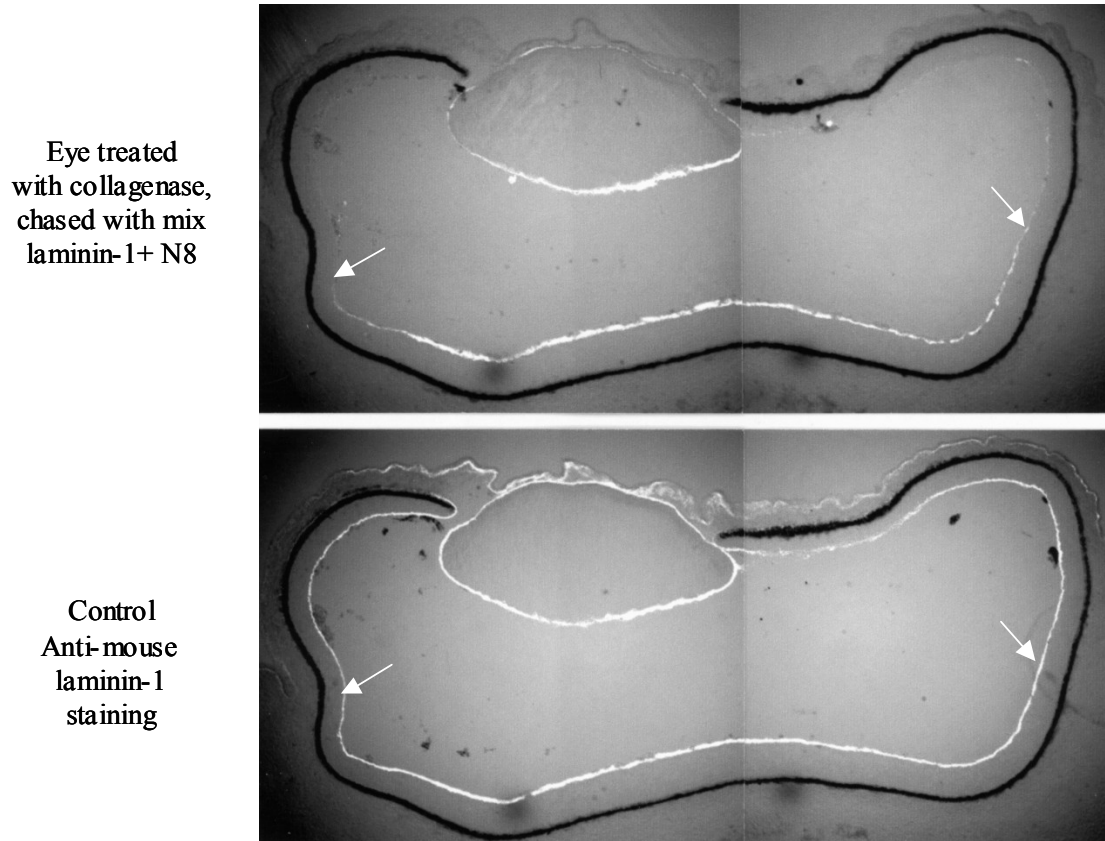


Figure 19 Laminin-chase experiment, the eye was injected with collagenase at E4, and chased 10 hours later with mouse laminin-1 plus N8; laminin-1 (conc: 2mg/ml, mixed 1:1 with the peptide). The embryo was sacrificed 24 hours later. Staining of the experimental eye with a monoclonal antibody (MAb) to c-myc shows that N8 got incorporated into the newly formed basal lamina until the complex of laminin-1 and N8 was depleted. Staining against mouse laminin-1 shows that mouse laminin-1 got incorporated during the whole regeneration process.

The retinal basal lamina was dissolved by collagenase and its regeneration was induced by the injection of laminin-1 pre-incubated with N8. The final concentration of laminin-1 was 1 mg/ml that of N8 was 0.15 mg/ml. 24 hours after injection a new basal lamina had been established over the whole surface of the retina as shown by anti-mouse laminin-1 staining (Figure 19b). Anti-myc staining revealed that N8 was incorporated into the new basal lamina indicating a stable complex between N8 and laminin-1 (Figure 19a). The pattern of the anti-

3. Results

myc staining with a strong staining in the center and a trailing staining towards the periphery of the retina (arrows) indicated that the N8/laminin-1 complex was preferentially incorporated as compared to laminin alone.

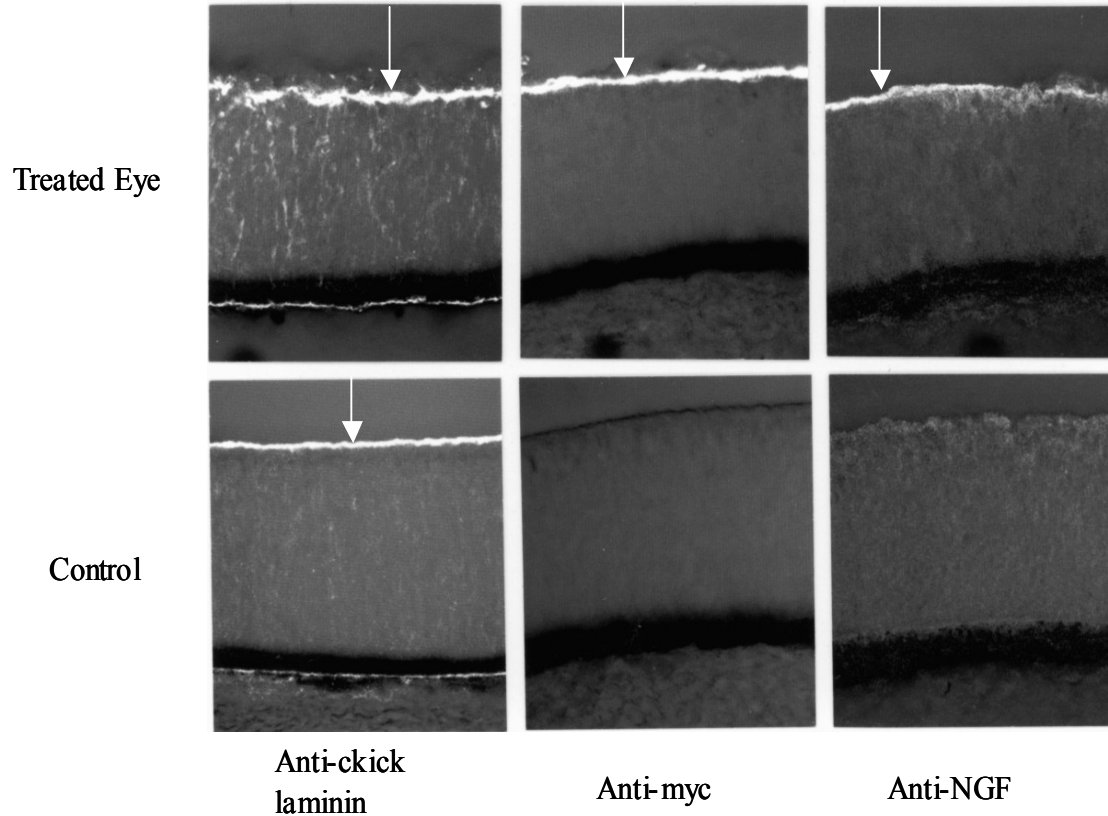


Figure 20 A closer look at the newly generated basal lamina after collagenase treatment and laminin-1 chase. In the treated eye (upper row) the anti-chick laminin staining reveals the position of the newly formed basal lamina. The anti-myc and the anti-NGF staining of peptide N8 reveal that the fusion protein was incorporated into the newly generated basal lamina. Anti-myc and anti-NGF staining are co-localized showing that the myc- as well as the NGF-Tag is immunoreactive.

A detailed look at the newly generated basal lamina revealed that peptide N8 got incorporated into the newly formed basal lamina. The myc-tag as well as the fused NGF-moiety on the peptide remained immunoreactive (Figure 20). A neurite outgrowth assay to determine the biological activity of the fused NGF moiety failed because the unfused proteins already displayed neurite outgrowth promoting activity.

3.3 Glycosylation of agrin

3.3.1 Expression of N-terminal agrin fragments

The coding sequence of agrin includes 20 SG sequences as potential GAG glycosylation sites. Of these, sites 5, 6, 11, 13, 16 and 20 are part of a more defined SGXG consensus sequences as candidate sites for GAG attachment. One of the SG sites, located between the 7th and 8th follistatin-like (FS) domain, and another in a serine/threonine-rich (S/T) domain, have multiple consensus sequences (Figure 1). In both sites, the SGs are separated by not more than 5 amino acids, with the exception of SG #10 which is separated from SG #9 by 7 amino acids. To determine which sites actually carry GAG chains, overlapping agrin fragments were expressed in eucaryotic cells, and the expressed peptides were investigated for GAG glycosylation. Three criteria were used to determine the presence of GAGs in the peptides: First, GAG-containing peptides usually run on SDS-PAGE as long smears rather than sharp bands. Second, digestion with heparitinase or chondroitinase should result in a major drop of the molecular weight that is clearly evident after SDS-PAGE. Third, the GAG glycosylated peptides should bind to anion exchange beads and elute only at ionic strength equal or higher than 1 M NaCl. Efforts were concentrated on agrin segments from the N-terminus to the first LG domain, because previous studies have already shown that the C-terminal LG domains of agrin are not GAG glycosylated (Denzer *et al.*, 1995). A diagram of agrin with its different domains is shown in. The peptide fragments (PF1-9) expressed for this study are also listed in Figure 9. They included the N-terminal half of the N-terminal agrin domain (NtA) (PF1), the C-terminal half of the NtA and FS modules 1 to 6 (PF2), FS 7 to the end of the S/T domain (PF3), the module first found in sea urchin sperm protein (SEA) up to the first epidermal growth factor like module (EGF)(PF4), the NtA and the first FS domain (PF5), FS domains 2 to 8 (PF6), the laminin EGF-like module (LE) up to the end of the first S/T domain (PF7), the NtA alone (PF8) and FS 1-8 (PF9).

The recombinant proteins were purified from cell culture supernatants of transfected EBNA cells and analyzed by SDS-PAGE followed by Western blotting. The protein sizes ranged from 25 to 200 kDa (Figure 10). Four of the fragments, PF3, PF6, PF7 and PF9, showed the high molecular

3. Results

weight smear typical for proteoglycans (Figure 10). All 4 fragments included at least one of the two clusters of tightly spaced SG consensus sequences found in the deduced amino acid sequence of the agrin cDNA sequence (Figure 1). In contrast to PF3, PF6, PF7 and PF9, the other fragments ran as sharp bands, according to their calculated molecular weights. Thus candidate sites for GAG attachment were indeed the clusters of SG consensus sequences between the 7th and 8th FS domain (site 1) and the end of the S/T domain further C-terminal (site 2).

The expressed PF7 and PF9 peptides, each of which carried one of the two multi-SG sequences, were fractionated on Q-Sepharose yielding 3 fractions: a flow-through, a low salt eluate and a high salt eluate. The flow-through was further purified using a cobalt based affinity column to absorb the His₆-tagged peptides. SDS-PAGE revealed that the peptides had a molecular weight of about 65 kDa, representing the core proteins of PF9 and PF7 (Figure 21, lanes 3 and 6). The 0.5 M low salt eluate showed a broad band that ranged from 65 to 180 kDa and represents a mixture of core protein, hypoglycosylated and fully glycosylated peptides (Figure 21, lane 1 and 4). The 1.5 M salt eluate appeared on the Western blots as long smears with molecular weights between 90 and 200 kDa, most likely representing the peptides with their attached GAGs (Figure 21, lanes 2 and 5). Quantification of the 3 fractions showed that approximately 30% of the expressed peptide was non-glycosylated core peptide, 30% was GAG-peptide and 40% was hypoglycosylated peptide.

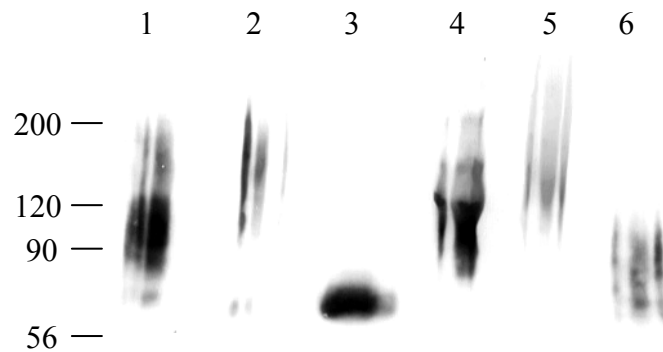


Figure 21 Western blot showing that the recombinant agrin peptides, PF9 (lanes 1-3) and PF7 (lanes 4 to 6), derived from the supernatants of HEK293/EBNA cells can be separated into three fractions by binding to Q-Sepharose. The flow-through (lanes 3 and 6) represents the core peptide of PF9 and PF7. The 0.5 M salt eluate (lanes 1 and 4) is a mixture of core protein, hypoglycosylated peptide and GAG glycosylated peptide. The 1.5 M salt eluate runs as a broad smear and represents the peptide with the GAG sidechains attached (lanes 2 and 5). A small amount of core protein was also detected in this fraction for PF9 (lane 2).

3. Results

Evidence that GAGs were attached to PF9 and PF7 came from experiments digesting the peptides with heparitinase and chondroitinase. When the high salt eluate of PF9 was digested with heparitinase its molecular weight dropped and the labeled band became much more defined (Figure 22, compare lanes 1 and 3). Digestion of PF9 with chondroitinase showed no major drop in molecular weight relative to the undigested peptide (Figure 22, compare lanes 1 and 2), indicating that PF9 carries heparan sulfate sidechains.

When PF7 was treated with the enzymes, its molecular weight dropped after treatment with chondroitinase (Figure 22, compare lanes 4 and 5) but not after heparitinase treatment (Figure 22, compare lanes 4 and 6). A slight increase in the amount of core protein after heparitinase treatment indicates that a minor part of the peptides carry HS sidechains. This shows that PF7 carries CS sidechains with a minor contribution of HS. In comparison, agrin from chick vitreous body showed a drop in molecular weight after heparitinase but not after chondroitinase treatment, confirming previous data (Denzer *et al.*, 1995; Tsen *et al.*, 1995) showing that agrin is a heparan sulfate proteoglycan (Figure 22, lanes 7-9).

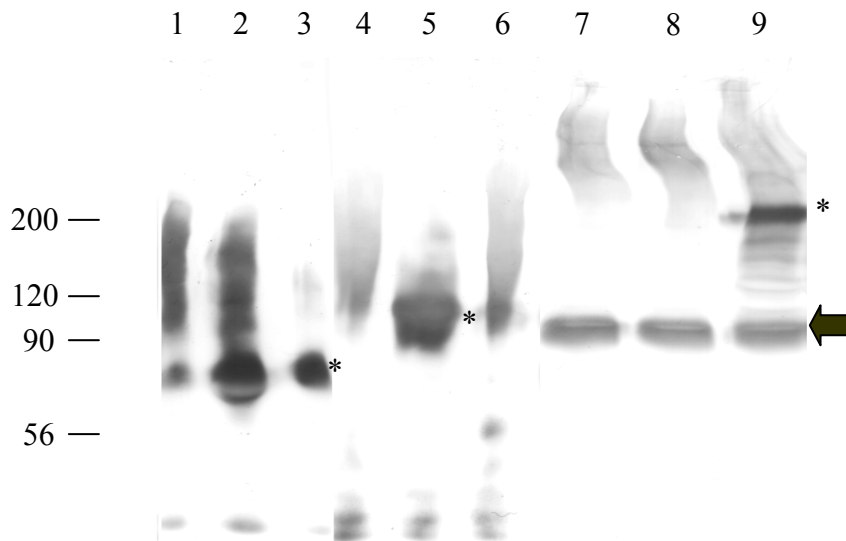


Figure 22 Western blot confirming that the high salt fraction of agrin fragments PF9 and PF7 are indeed proteoglycans. The untreated peptides ran as long smears as shown in lanes 1 and 4. Treatment of PF9 peptide with chondroitinase does not lead to a major change in the banding pattern relative to the untreated control (compare 1 and 2), whereas treatment with heparitinase leads to a major drop in the molecular weight of the labeled peptide (lane 3). Treatment the PF7 peptide with chondroitinase leads to a drop in molecular weight and a sharpening of the labeled band (lane 5), whereas treatment with heparitinase has no effect on the banding pattern of the peptide (lane 6). However, there was a slight increase in the amount of core protein (lane 6), suggesting a minor part of the GAG of PF7 being HS. Agrin from vitreous body runs as a diffuse band at 400 kDa (lane 7). The diffuse banding remains after treatment with chondroitinase (lane 8), whereas treatment with heparitinase results in a major drop of agrin immunoreactivity to 200 kDa (lane 9). The band at 90 kDa is a naturally occurring C-terminal agrin fragment in vitreous body (arrow). The stars indicate the core proteins.

3. Results

3.3.2 Localization of the GAG attachment sites in PF9

To locate the SGs responsible for the GAG attachment in PF9 the serines of the triple SG consensus sequences of PF9 were changed to alanines by site-directed mutagenesis, and the mutated peptides were expressed in HEK293/EBNA cells. SDS-PAGE followed by Western blotting showed that the exchange of individual serines in the triple SG cluster did not alter the molecular weight of the core protein (Figure 23). Further, every mutated peptide showed a long smear above the core protein indicating GAG glycosylation of every mutant peptide as well as the unmutated peptide (Figure 23, lanes 1-4). However, the trail of glycosylated peptide was reduced in size from 200 to 150 kDa in all mutations (Figure 23, lanes 2-4). Double-mutations of serines in any permutation did not cause an additional shift in the molecular weight (Figure 23, lanes 5-7), indicating that any of the SGs is equally capable of carrying the GAG sidechains. Absence of the GAG glycosylation trail of the protein was only observed after the elimination of all 3 serines in the SG cluster (Figure 23, lane 8).

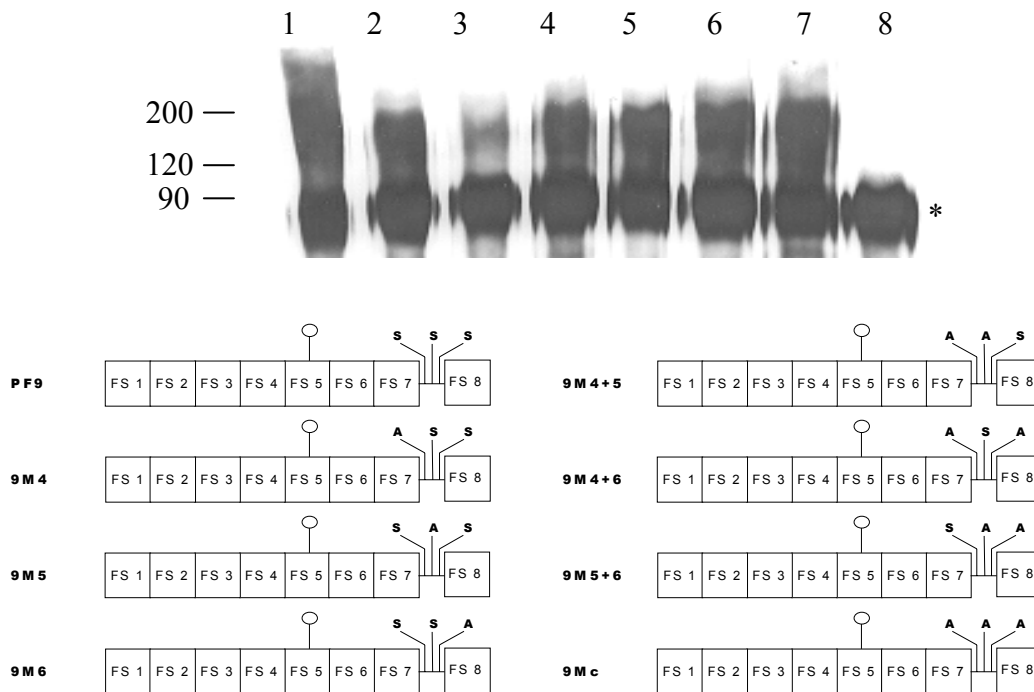


Figure 23 Western blot showing PF9s after site-directed mutagenesis to exchange various serines in the SG cluster. The non-mutated peptide is shown in lane 1. Lanes 2 to 4 show the peptides after the mutation of the individual S to alanines. The diagrams below show the location of the mutations and the presence of the remaining SGs. Lanes 5 to 7 show the peptides expressed after double-mutation of two of the three serines. Lane 8 shows the peptide after the mutation of all 3 serines in the PF9 peptide. The GAG glycosylated smear only disappears after the mutation of all three serines in the PF9 peptide. The stars indicate the core proteins.

3. Results

To identify the type of GAGs attached to PF9 and in each of the serine-to-alanine mutations, the peptides were digested with chondroitinase or heparitinase. Molecular weight changes were observed after heparitinase treatment (Figure 24, lanes 3 and 6) but not after treatment with chondroitinase (Figure 24, lanes 2 and 5), showing that the GAGs in the mutations of PF9 were HS and not CS sidechains. That was true for all single and double mutations (Table 4).

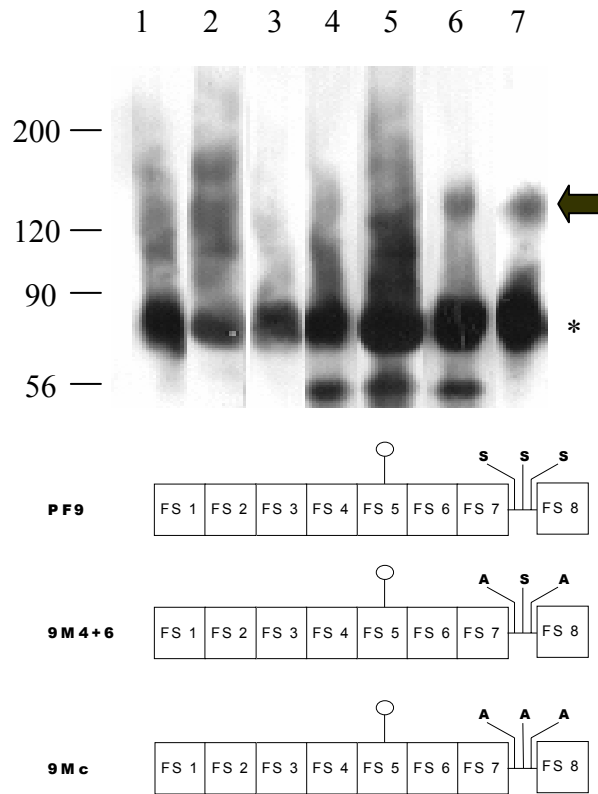


Figure 24 Western blots defining the GAG sidechains attached to FP9 and its mutated versions. The non-mutated peptide is shown in lane 1. Treatment of the peptide with chondroitinase had no effect on the banding pattern, whereas heparitinase led to a major reduction of the high molecular smear, indicating that PF9 is a HSPG. The digestion of the double-mutant peptide (lane 4) with chondroitinase (lane 5) and heparitinase (lane 6) showed that the high molecular smear was unaffected by chondroitinase (lane 5), but was greatly reduced after heparitinase treatment (lane 6). The triple mutated peptide that has no GAG chains is shown in lane 7 for comparison. The band indicated by the arrow most likely represents the peptide dimer (Wiberg *et al.*, 2001) and was detected in both the heparitinase-digested as well as in the fully mutated version of the peptide (compare lane 6 and 7).

3. Results

Table 4 Amino acid sequence of the SG clusters in the expressed PF9 peptide and its mutations. The sensitivity to heparitinase and chondroitinase is shown in the right columns. A scale from 0-5 was used to describe the sensitivity of the peptides to treatment with the corresponding enzyme (with 5 meaning: very sensitive and 0: no effect at all).

construct	potential GAG site	Sensitive to CS	Sensitive to HS
PF9	EDEC GS ⁶⁴⁸ GG S ⁶⁵¹ GS ⁶⁵³ GDGSECEQD	0	5
9M4	EDEC GA ⁶⁴⁸ GG S ⁶⁵¹ GS ⁶⁵³ GDGSECEQD	0	5
9M5	EDEC GS ⁶⁴⁸ GGA ⁶⁵¹ GS ⁶⁵³ GDGSECEQD	0	5
9M6	EDEC GS ⁶⁴⁸ GG S ⁶⁵¹ GA ⁶⁵³ GDGSECEQD	0	5
9M4+5	EDEC GA ⁶⁴⁸ GGA ⁶⁵¹ GS ⁶⁵³ GDGSECEQD	0	5
9M4+6	EDEC GA ⁶⁴⁸ GG S ⁶⁵¹ GA ⁶⁵³ GDGSECEQD	0	5
9M5+6	EDEC GS ⁶⁴⁸ GGA ⁶⁵¹ GA ⁶⁵³ GDGSECEQD	0	5
9Mc	EDEC GA ⁶⁴⁸ GGA ⁶⁵¹ GA ⁶⁵³ GDGSECEQD	no GAG	no GAG

3.3.3 Localization of the GAG attachment sites in PF7

Similar to PF9, switches of individual serines in the SG cluster of PF7 to alanines did not cause a major shift in molecular weight of PF7 and did not result in a loss of the high molecular weight smear typical for the presence of GAGs (Figure 25, lanes 1 to 5). However, a reduction in size was observed in double (Figure 25, lane 6) and triple mutations of the 4 serines (Figure 25, lane 7). A total loss of the carbohydrate smear was only observed after mutating all 4 serines in the SG cluster of PF7 (Figure 25, lane 8).

Digestion of PF7 and the individual mutant peptides showed that the GAG attached to this fragment was predominantly CS with a minor contribution of HS (Figure 26; Table 5). The HS sidechain was no longer detectable in single, double and triple mutations affecting serine # 11 (Table 5).

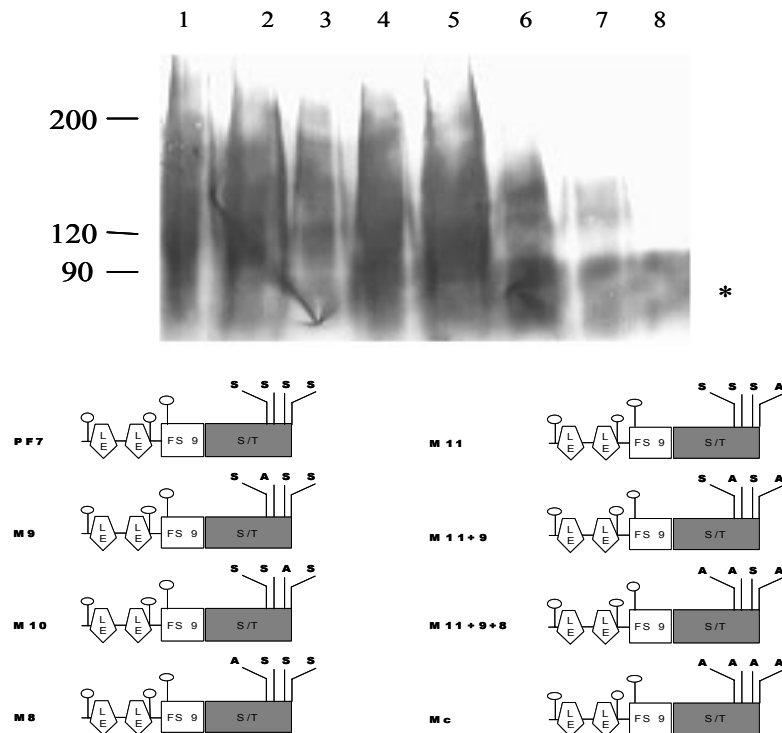


Figure 25 Western blot showing PF7s after site-directed mutagenesis to exchange various serines in the SG cluster. The non-mutated peptide is shown in lane 1. Lanes 2 to 5 show the peptides after the mutation of the individual serines to alanines. The diagrams below show the location of the mutations and the presence of the remaining SGs. Lanes 6 to 7 show the peptides expressed after the mutation of 2 and 3 of the 4 serines. Lane 8 shows the peptide after the mutation of all four serines in the SG cluster. The GAG glycosylated smear only disappears after the mutation of all four serines in the PF7 peptide. The star indicates the core proteins.

3. Results

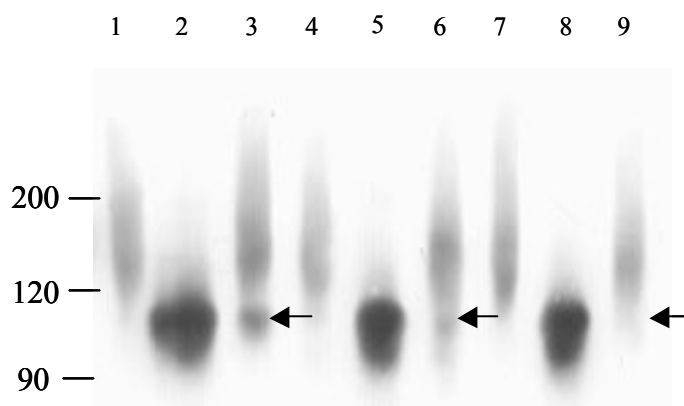


Figure 26 Western blots defining the GAG sidechains attached to FP7 and its mutated versions. The non-mutated peptide is shown in lane 1. Treatment of the peptide with chondroitinase led to a major reduction of the high molecular smear (lane 2), whereas treatment with heparitinase had little effect on the banding pattern of the peptide (lane 3). However, a slight increase of core protein (arrows) after enzyme treatment was detectable. The peptide with an exchange of serine 8 to alanine ran as a long smear (lane 4) that was reduced only after treatment with chondroitinase digestion (lane 5), but not after treatment with heparitinase (lane 6). A minor increase of core protein was detectable after heparitinase treatment. The mutation of serine 11 to alanine also appeared a long smear (lane 7) that disappeared after chondroitinase (lane 8) but not after heparitinase (lane 9) treatment. Treatment with heparitinase did not result in an increase of core protein for this mutation and all mutations affecting this particular serine.

Table 5 Amino acid sequence of the SG clusters in the expressed PF7 peptide and its mutations. The sensitivity to heparitinase and chondroitinase is shown in the right columns. A scale from 0-5 was used to describe the sensitivity of the peptides to treatment with the corresponding enzyme (with 5 meaning: very sensitive and 0: no effect at all).

construct	potential GAG site	Sensitive to CS	Sensitive to HS
PF7	ES ¹⁰⁴⁹ GSAEGS ¹⁰⁵⁵ GDQEMSI ¹⁰⁶³ GDQESS ¹⁰⁶⁹ GAGSAGEEEVEE	5	2
7M9	ES ¹⁰⁴⁹ GSAEGA ¹⁰⁵⁵ GDQEMSI ¹⁰⁶³ GDQESS ¹⁰⁶⁹ GAGSAGEEEVEE	5	2
7M10	ES ¹⁰⁴⁹ GSAEGS ¹⁰⁵⁵ GDQEMSI ¹⁰⁶³ GDQESS ¹⁰⁶⁹ GAGSAGEEEVEE	5	2
7M8	EA ¹⁰⁴⁹ GAAEGS ¹⁰⁵⁵ GDQEMSI ¹⁰⁶³ GDQESS ¹⁰⁶⁹ GAGSAGEEEVEE	5	1
7M11	ES ¹⁰⁴⁹ GSAEGS ¹⁰⁵⁵ GDQEMSI ¹⁰⁶³ GDQEAA ¹⁰⁶⁹ GAGSAGEEEVEE	5	0
7M11+9	ES ¹⁰⁴⁹ GSAEGA ¹⁰⁵⁵ GDQEMSI ¹⁰⁶³ GDQEAA ¹⁰⁶⁹ GAGSAGEEEVEE	5	0
7M11+9+8	EA ¹⁰⁴⁹ GAAEGA ¹⁰⁵⁵ GDQEMSI ¹⁰⁶³ GDQEAA ¹⁰⁶⁹ GAGSAGEEEVEE	5	0
7Mc	EA ¹⁰⁴⁹ GAAEGA ¹⁰⁵⁵ GDQEMSI ¹⁰⁶³ GDQEAA ¹⁰⁶⁹ GAGSAGEEEVEE	no GAG	no GAG

3.4 Neurite outgrowth inhibition by agrin

Previous studies have shown that full-length agrin, as well as a N-terminal 150 kDa fragment of agrin inhibited neuron outgrowth of ciliary ganglia (CG) neurons *in vitro*, while a C-terminal 95 kDa fragment had no influence on neurite outgrowth (Bixby *et al.*, 2002). These findings imply that the N-terminal domains of agrin are responsible for this effect. To determine the domains of agrin responsible for neurite outgrowth inhibition, various fragments of the N-terminal domains of agrin (Figure 9) were subject to an *in vitro* assay utilizing dorsal root ganglia (DRG). To test the influence of GAG chains in this matter, fragments containing GAG chains, as well a mutant of the same fragment without GAG chains were tested in this assay.

For these experiments dissected DRGs were cultured on a laminin-1 (LN) substrate (20 µg/ml laminin-1) adjacent to a “stripe” of test substrate (20 µg/ml laminin-1 plus 3 µl peptide (360 nM)). On the LN substrate alone, DRG neurites grew extensively. When neurites passed from one LN substrate to an adjacent LN substrate the outgrowth pattern was indistinguishable (Figure 27; LN/LN). No change in the neurite-promoting effect was visible when the neurites reached the test-stripe containing PF5/LN (Figure 27; PF5). The same was true for peptides PF1-, PF2-, PF4-, PF5-, and PF8/LN. A stripe containing fragments PF3-, PF7-, and PF9/LN however, showed inhibitory effects on the dorsal root ganglia neurites (see Figure 27 and Figure 28). PF3 contains the two multiple SG-consensus sequences shown to be able to carry glycosaminoglycan sidechains (see chapters 3.3 and 4.3) while PF7 and PF9 each just contain one of these sites. To determine if in fact the GAG chains are the determining factor for this effect fragments 9Mc and 7Mc (the mutated fragments that are not capable of carrying GAG chains, see Figure 23 and Figure 25) were used in the test-substrate. Deletion of the GAG-attachment sites in PF9 led to a loss of neurite inhibition for this peptide. The same was true for the mutation of GAG attachment sites in PF7 (Figure 28; PF7 mutant).

3. Results

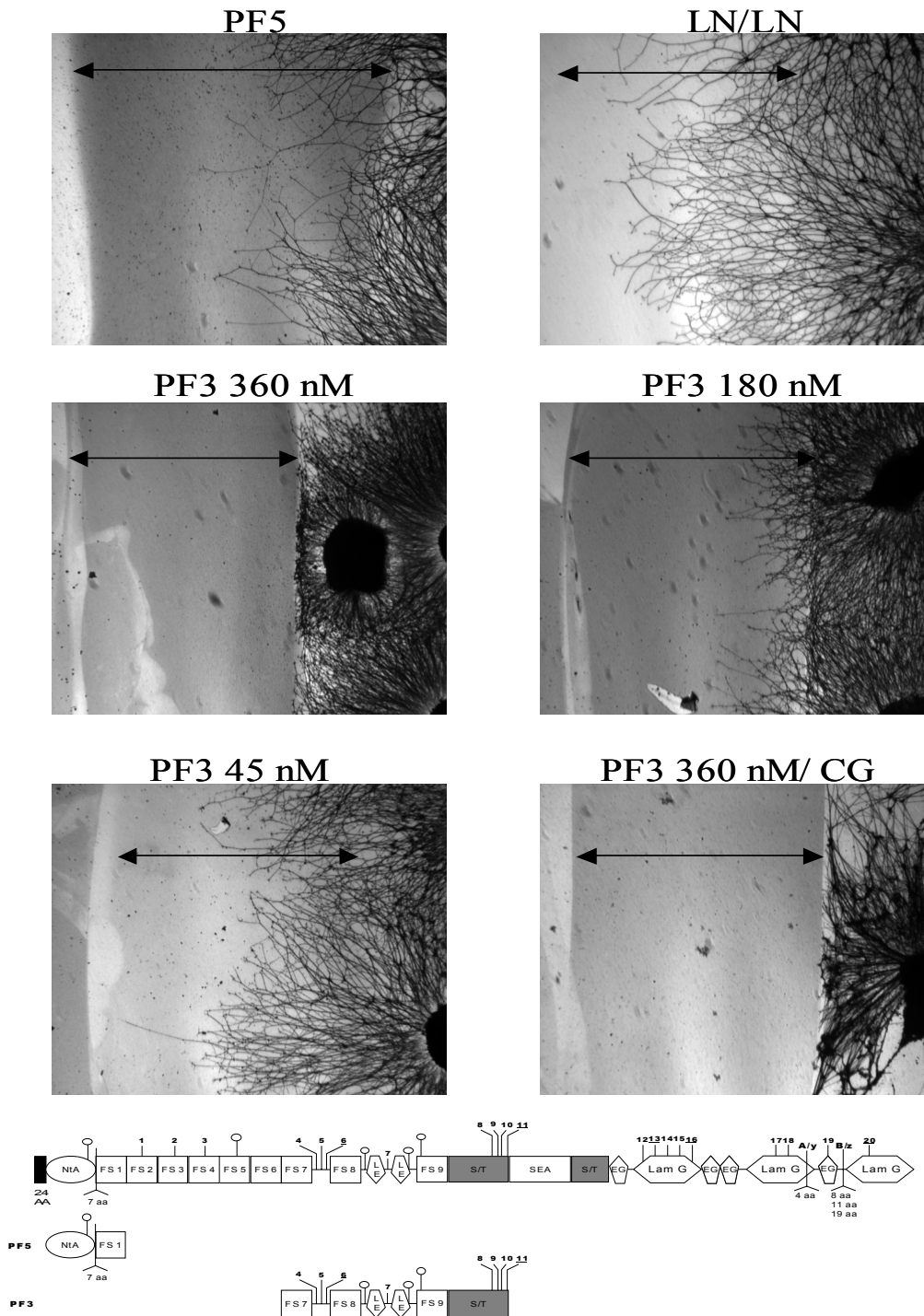


Figure 27 Neurite outgrowth assay. Upper left: PF5 was used as control at a concentration of 360 nM. Upper right: another control showing that the laminin-strip without a peptide does not change the neurite outgrowth pattern. Middle and bottom row: PF3 in different concentrations, showing that PF3s capability to inhibit neurite outgrowth is strongest at a concentration of 360 nM and no inhibition was found for a concentration of 45 nM. Bottom right: showing that the findings are also true for the use of ciliary ganglia.

3. Results

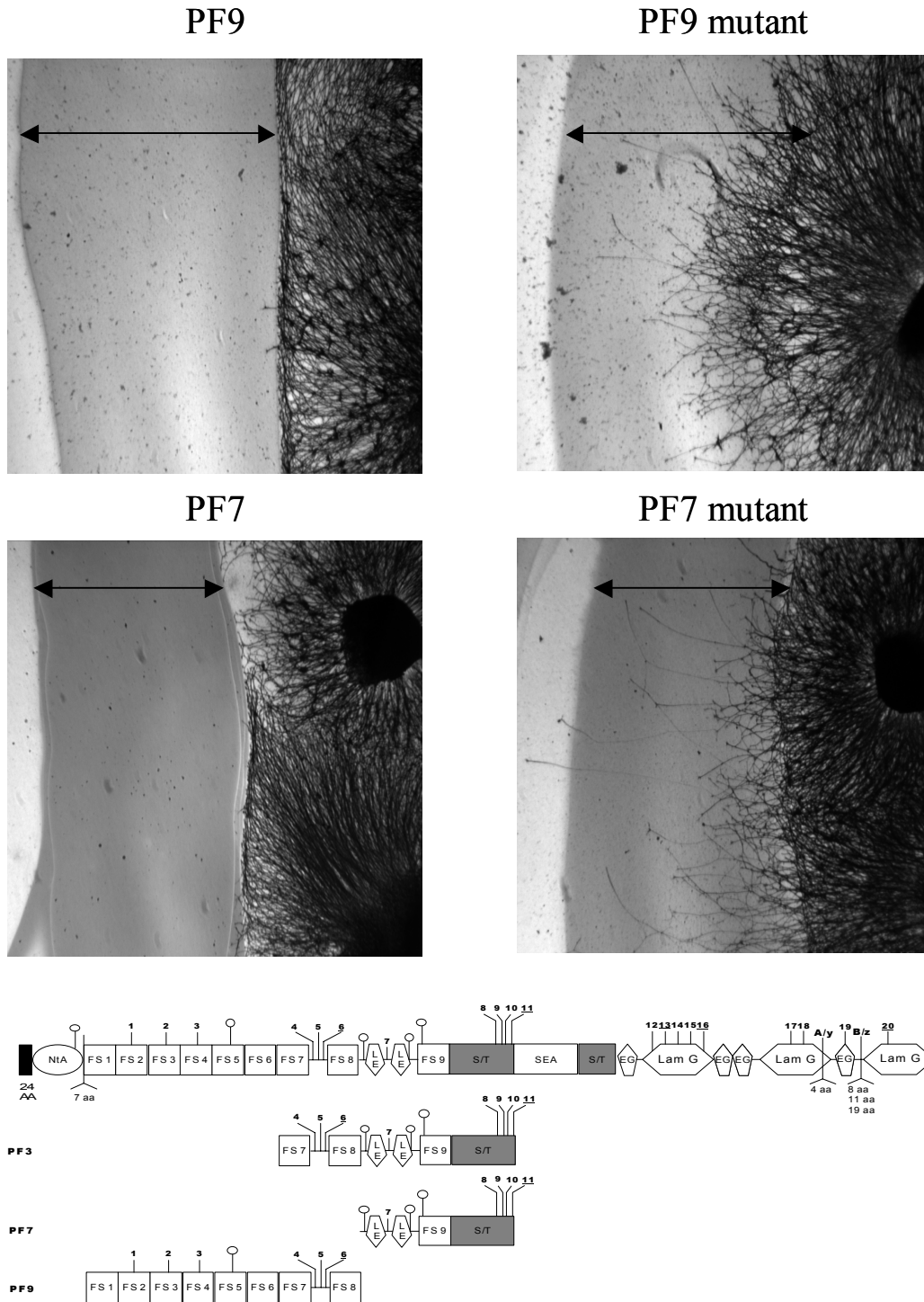


Figure 28 Neurite outgrowth assay. Top row: PF9 and the mutated 9Mc at a concentration of 360 nM. Bottom row: PF7 and the mutated 7Mc at a concentration of 360 nM.

4. Discussion

4.1 Binding to laminin-1

The interaction between laminin-1 and agrin is essential for synapse formation in the peripheral nervous system and in particular in muscle (Burgess *et al.*, 2000). It may also play a role in other places of the extracellular matrix for stabilization and interactions of basement membranes (Burkin *et al.*, 2000; Sugiyama *et al.*, 1997). The agrin-binding site was determined to be located in the central region of the long arm of laminin-1. The binding site maps to 20 residues within the γ 1-chain of laminin-1 and requires the native coiled-coil conformation (Kammerer *et al.*, 1999). It may be expected from these data, that agrin binds to all laminins containing the γ 1 chain with variations in affinity imposed by the other chains. Laminin-1 is an embryonic form of the laminins (Ekblom, 1981), whereas laminin-2 and -4 are found in later stages of skeletal myogenesis. These three laminins contain the γ 1-chain (Timpl and Brown, 1994). No binding is therefore expected to laminin-5 with its γ 2 chain or to laminin-12 with its γ 3 chain (Koch *et al.*, 1999), because of the non-conserved binding motif in γ 2 and γ 3. Furthermore binding was shown to be strongest to laminin-4 followed by laminin-1 and laminin-2 (Denzer *et al.*, 1997).

To demonstrate that the NtA-domain is sufficient to mediate laminin-1 binding, binding activities of single NtA and NtA-FS were compared and revealed identical values for both proteins. Together with the mutation that prevented N-glycosylation of the NtA-domain these experiments clearly indicate that the high affinity protein-protein interaction ($EC_{50} \sim 5$ nM) is mediated exclusively by the NtA, without involvement of the carbohydrate chains (Mascarenhas *et al.*, 2003). *In vivo* experiments involving injection of the laminin-binding protein fragments into the vitreous of chick embryos as well as collagenase/laminin-1 chase experiments verified the results obtained from the *in vitro* studies. Another observation was that a complex of laminin-1 with PF8 (NtA) was preferably incorporated into the newly formed basal lamina.

4. Discussion

Examination of the conformation of the 20 amino acid stretch of the γ 1-chain within the coiled-coil domain of laminin-1 revealed that there are a number of negatively charged amino acids on the surface of the coiled-coil domain, which would be available for ionic interactions. Therefore the assumption of an interaction with positively charged amino acids within the NtA-domain seems likely. For this approach highly conserved positively charged amino acids (K and R) within the NtA were chosen for site-directed mutagenesis. The discrepancy of up to 100% between independent measurements in the solid phase binding assay can be explained with inaccuracies during the preparation of the dilution series (which is very sensitive in nM range). A definite decrease of binding activity was found for mutations M43 (R43A) and M111 (R111A). Mutation M4,5,9 (RRR4,5,9AAA) showed a slight decrease of binding activity as well, which seems a contradiction to the findings of Mascarenhas. *et al.*, that showed that deletion of helix1 does not have an influence on NtA's binding property. But assuming that the triple mutation within helix-1 destroys its 3-D structure (even though not detectable by limited tryptic digest) and therefore could interfere with the underlying "groove" between the β -barrel fold and helix3 may explain this phenomenon.

R111 is one of the center amino acids of the linkage-arm between the β -barrel core and the α -helix3. This linkage is probably important to arrange helix-3 in the right position and assure correct distance between the helix-3 and the core to form the groove that is necessary for laminin binding. It remains unclear if the function of R111 is to assure correct 3D structure of the NtA, or if it serves as binding partner in an ionic interaction with negatively charged amino acids of the laminin coiled-coil domain. The very low expression rate of the protein could indicate that this protein is not stable, which would emphasize the importance of the amino acids in the linker region between β -barrel core and helix-3. One way to address the open questions in this case would be to co-crystallize the NtA-domain and a protein fragment containing the relevant part of the laminin coiled-coil domain.

The data obtained from this work can be discussed best with the knowledge of the results of an overlapping study, which was conducted at the same time by Mascarenhas *et al.* The mutagenesis experiments performed by the researchers were based on the knowledge

4. Discussion

of the exact three dimensional structure of the NtA-domain and commenced on the basis of potential sites proposed in the work of Stetefeld *et al.* (Stetefeld *et al.*, 2001).

The interpretation of the mutagenesis data in context with the crystal structure of chicken NtA indicated a major primary effect for the mutation of 2 hydrophobic amino acids in α -helix 3 (L117 and V124) and a minor secondary effect for mutations of charged amino acids (lower part of a cluster of charged amino acids and R43) on the surface of the β -barrel fold facing the groove between the β -barrel core and α -helix 3. While single mutations of the hydrophobic amino acids in α -helix 3 resulted in strong decrease of binding (60-100 fold), the influence of the charged amino acids seemed rather weak (20-40 fold decrease). The two crucial amino acids are located on the same site of α -helix 3, facing the groove between the β -barrel core and α -helix3 (“barrel face”).

A comparison of laminin sequences of γ -chains from mouse, rat and human within the mapped binding region of the NtA shows that this region is highly conserved for γ 1-, but rather divergent for γ 2- and γ 3-chains (Mascarenhas *et al.*, 2003). Previous studies have demonstrated that the γ 2-chain of laminin is not effective in competition assays with laminin-1 (Kammerer *et al.*, 1999).

Using a computer-model it was shown that the distance between L117 and V124 (10.6 Å) matches the distance of the 7-residue interspace between A1305 and A1312 (10.7 Å) of the laminin γ 1-chain. Therefore an interaction seems quite possible. Based on this assumption, D1308 and E1315 would be placed in close proximity to R43 and R40 of the NtA-domain, which would support the idea of an ionic interaction. Based on these data the laminin binding is due to a combination of hydrophobic and ionic interactions.

It cannot be excluded that other interactions of the NtA-domain with either the α - or β -chain of laminin exist.

4.2 Fusion protein with NGF

The use of peptide signaling molecules such as growth factors for clinical applications is extremely limited by the low target specificity of these molecules and their short half-lives *in vivo*. Some efforts have been made to create fusion proteins that would make those molecules more convenient for clinical applications. The present study was aimed to utilize the laminin-binding domain of agrin (NtA) as an anchoring unit for the nerve growth factor.

For this purpose NGF-mature was fused to the C-terminal end of the laminin-binding peptides PF5 (NtA + FS) and PF8 (NtA) of agrin. In the case of PF5 + NGF (N5) no difference between the binding activity of PF5 and N5 were notable. In the case of N8 however a slight decrease in binding activity to laminin-1 was detectable. This may be caused by spherical interference between NGF and the NTA-domain. In N5 the additional FS-domain may function as a spacer between the NtA and NGF and hence prevent interference between these two domains. *In vivo* experiments confirmed the findings established in the solid phase binding assay, showing that the NtA-domain can be used for anchoring molecules to the basal lamina.

The growth factor activities of the fusion proteins were not stronger than the activity of the unfused PF5 or PF8. The impaired growth factor activity of the fusion proteins may be caused by interference between the laminin-binding domain and the NGF receptor and/or misfolding of the NGF moiety itself. This problem may be correctable with the insertion of additional amino acids that act as a “spacer” between the laminin-binding coiled-coil domain and the growth factor moiety.

4.3 Glycosylation of agrin

4.3.1 GAG attachment sites of agrin

The present study localized the GAG attachment sites of agrin to two sites of the protein. Both sites have clusters of three and four closely spaced SGs next to each other. Only three out of seven sites are consistent with the SGXG consensus sequence that was supposed to predict the presence of GAG attachment sites in a core protein. Three other SGXG sites of agrin were not GAG glycosylated, questioning the validity of this consensus sequence as a predictor for the presence of GAG in a protein. By comparing the identified GAG attachment sites of agrin with the GAG attachment sites in perlecan (Dolan *et al.*, 1997) and collagen XVIII (Dong *et al.*, 2002), the other two basement membrane HSPGs, several rules for the prediction of GAG attachment sites could be established. First, repetitive SGs in short sequence are excellent candidate sites for HS attachment. Second, a series of acidic amino acids in front and/or the back of a SG cluster is another indicator for GAG glycosylation. Finally, by comparing the amino acid sequences for all attachment sites of agrin, perlecan and collagen XVIII, the most common consensus sequence associated with a HS sidechain was Gly (Ala)-Ser-Gly (Figure 29).

4. Discussion

1	VRSA <u>D</u> GQTAGCVC PASC <u>SG</u> VA <u>E</u> SIVCGS <u>D</u> GK <u>D</u> YRSE <u>C</u> ²⁹⁸	} Agrin	
2	VMGRTGAIRGL <u>E</u> IQKVR <u>SG</u> QCQH <u>D</u> KCK <u>D</u> ECKFN <u>A</u> VC ⁴⁰⁷		
3	<u>E</u> RQKA <u>E</u> CHQKAAI PVKH <u>SG</u> PC <u>D</u> LGTPSPCLSV <u>E</u> CTFG ⁴⁷⁸		
4*, <u>5</u> *, <u>6</u> *	QKSI <u>E</u> VAKMGPC <u>E</u> DECG <u>SG</u> <u>SG</u> <u>S</u> G <u>D</u> SE <u>C</u> E <u>Q</u> DRCRHY ⁶⁹¹		
7	RCEPGFWNFRGIVT <u>D</u> SK <u>SG</u> CTPCNCDPVGSVR <u>D</u> DCE <u>Q</u> ⁸⁶¹		
8*, 9*, 10*, <u>11</u> *	YA <u>E</u> SGSA <u>E</u> SG <u>D</u> Q <u>E</u> MSI <u>SG</u> <u>D</u> Q <u>E</u> S <u>SG</u> AGSAGE <u>E</u> EE <u>V</u> EE <u>S</u> ¹¹⁰⁶		
12	KAYHTVRIAMEFRATE <u>EL</u> SGLLLYNQNRGK <u>D</u> F ¹⁴³⁶		
<u>13</u>	ISLALVGGF <u>V</u> ELRFNTG <u>SG</u> TGVTTSKVR <u>V</u> EP ¹⁴⁶⁷		
14, 15	VNRNRR <u>SG</u> MLAV <u>D</u> GEHV <u>SG</u> ESPTGTDGLNL <u>D</u> TDLFV <u>G</u> ¹⁵¹¹		
<u>16</u>	NNQMY <u>D</u> LR <u>E</u> KGS <u>D</u> VLYG <u>SG</u> V <u>G</u> ECGNDPCHPNPCHHGA ¹⁵⁷⁷		
17	LTCRQMS <u>M</u> EVVFLAKSP <u>SG</u> MIFYNGQKT <u>D</u> GK <u>G</u> DFVSL ¹⁷⁰⁷		
18	SK <u>E</u> VPPLNTWISVLL <u>E</u> R <u>SG</u> RKGVMRINNGERVM <u>G</u> ES <u>P</u> ¹⁷⁶⁵		
19	TCS <u>P</u> RL <u>E</u> SY <u>E</u> CACQRGF <u>SG</u> AHCEKVII <u>E</u> KAAG <u>D</u> A <u>E</u> A <u>I</u> ¹⁸⁸⁴		
<u>20</u>	HF <u>E</u> LSIK <u>T</u> EATQGLILW <u>SG</u> K <u>G</u> LE <u>R</u> SDYIALAIV <u>D</u> GFV ¹⁹⁶⁶		
1	<u>E</u> LEEG <u>S</u> GLFVA ¹⁹⁹		} Collagen XVIII
2*, 3, 4	<u>E</u> EDDA <u>E</u> AS <u>G</u> DFG <u>SG</u> A <u>E</u> DRHHP <u>SG</u> K <u>D</u> KG ²⁵⁸		
5	PPV <u>E</u> GS <u>G</u> TRSS ²⁸²		
6, 7*	GPK <u>G</u> <u>D</u> SGT <u>SG</u> ILG ³³⁰		
<u>8</u> *	<u>I</u> D <u>M</u> EG <u>SG</u> F <u>G</u> <u>D</u> LE ⁴⁸¹		
9	FG <u>D</u> MEG <u>S</u> GLPLA ⁶²⁸		
<u>1</u> *, 2*, 3*	<u>D</u> DEDLLP <u>D</u> DA <u>SG</u> <u>D</u> GLG <u>SG</u> <u>D</u> VG <u>SG</u> ⁷⁷	} Perlecan	

Figure 29 Amino acid sequences of all 20 potential GAG attachment sites of agrin. The SG sites are aligned; the acidic amino acids are depicted in red. SGXG consensus sequences are underlined, and the confirmed GAG attachment sites are marked with a star. Every last amino acid in a line is numbered starting from the amino-terminal methionine. For comparison the consensus sequences for GAG attachment sites in collagen XVIII and perlecan are also shown.

The current data are consistent with a previous study postulating similar criteria to predict a potential HS attachment site, such as tightly packed repetitive SGs, and a nearby cluster of acidic amino acids (Zhang *et al.*, 1995).

While the criteria listed above make a particular site a good candidate, an unequivocal prediction for GAG attachment site is not possible. Several SG sequences in collagen XVIII that fulfill the above criteria are not glycosylated, and the prediction of CS versus HS attachment site is even more ambiguous. Evidence for the actual presence of a GAG at a

4. Discussion

particular site requires site-directed mutagenesis combined with *in vitro* expression of the mutant proteins. Yet, two more factors complicate the analysis. Expression of peptides instead of the entire protein may not replicate the GAG assembly that occurs in the intact protein. *In vitro* expression of agrin peptides, for example, led only in one of the two sites to the correct GAG. While one of the peptides containing one of the GAG attachment sites is connected to HS, the other one is incorrectly connected to CS, since agrin from embryos and full-length agrin expressed *in vitro* is a HSPG with no contribution of CS sidechains. It appears that sites distant to the SG clusters are additional determinants for the correct glycosylation confirming previous findings in perlecan and glypican (Chen and Lander, 2001; Dolan *et al.*, 1997). Another complicating factor is that the GAG glycosylation *in vivo* is not always correctly repeated *in vitro*. In the case of collagen XVIII, the *in vitro* expressed protein is a hybrid HSPG/CSPG, whereas the *in vivo*-derived collagen XVIII is exclusively a HSPG. In addition, it was found that the culture conditions for the HEK293 cells to express the recombinant proteins, such as addition of fetal calf serum, may also be an important factor in promoting glycosylation. This was, however, not the case for agrin, where agrin peptide expressed in serum-free or serum-containing medium was equally well glycosylated. Based on the limitations provided by protein expression systems *in vitro*, the final verdict for the precise identification of a PG must also include the analysis of the *in vivo*-derived protein.

Site-directed mutagenesis of individual or several of the SGs in the two agrin SG-clusters revealed two more interesting aspects. First eliminating 2 out of 3 or 3 out of 4 serines in the SG-clusters still primed the synthesis of HS sidechains. This implies that SG clustering is not an absolute requirement for HS priming. The clustering of SG might be a means to ensure glycosylation at these particular sites of the protein. This could have evolutionary reasons, to guarantee that even in case of a random point mutation of one of the serines, another serine in the cluster could carry the GAG.

Furthermore, the mutations experiments showed that all serines in a SG cluster are capable of carrying a GAG sidechain. There was no preference of glycosylation for a particular serine in any of the two SG clusters in agrin. In collagen XVIII, however, it was only the first serine in a cluster of three SGs that was glycosylated. The second serine in the collagen XVIII SG cluster was only important to direct the glycosylation for HS instead of CS and the third SG was not important to GAG priming at all (Dong *et al.*, 2002). An effect of adjacent SGs on the type of GAG glycosylation was not observed for the first multiple SG – site (PF9), since the GAG sidechains remained the same after mutations of the adjacent

serines. A minor shift of HS to CS was, however, observed for the second multiple SG site (PF7).

A question that was not resolved in the current project is whether the GAGs in a SG cluster of *in vivo*-derived agrin are connected to one particular SG or any of the SGs. The presence of glycosaminoglycan in all mutant peptides indicates that in the case one serine is missing the glycosyltransferases glycosylated the next best serine. It is also possible that each SG cluster of agrin carries just one GAG, and this GAG sidechain is randomly attached to any of the three or four serines. In the last case one would expect equal amounts of the three or four different glycosylation isoforms. The minimal size difference between non-mutated, singly and doubly-mutated peptides of PF9 indicates that each of the SG clusters carries only one GAG sidechain in the range of up to 100 kDa. In the case of PF7, the size of glycosylation is reduced in the double and triple mutations, suggesting that more than one GAG chain could be attached to the peptide. This is consistent with the fact that the size difference between glycosylated agrin and its core protein suggests 3-4 HS sidechains (Denzer *et al.*, 1995; Halfter *et al.*, 1997).

4.3.2 Function of GAGs in agrin

Agrin is a component of the extracellular matrix that is important for the organization of the neuromuscular junction during development. Targeted elimination of agrin results in neonatal death due to inability of mice to breath. Histological studies showed that in the absence of agrin, neuromuscular junctions do not form and nerve fibers do not innervate muscle fibers but show excessive growth into the tissues (Gautam *et al.*, 1996). Studies using a recombinant mini-agrin composed of the 3 C-terminal LG-domains and the NtA – domain was already sufficient to induce clustering of the AchRs (Meier *et al.*, 1998), showing that the GAG sidechains of agrin are not necessary for receptor aggregation. This raises the question of the purpose of the GAG chains in agrin. It has been shown previously that the binding of agrin to a series of ligands, receptors and growth factors is mediated by its HS sidechains. These include FGF-2, thrombospondin and receptor tyrosine phosphatase (Aricescu *et al.*, 2002; Cotman *et al.*, 1999).

Interestingly, agrin is a major component of senile plaques in dementia of the Alzheimer's type. By using solid-phase immunoassay, an interaction between agrin and the amyloidogenic peptide A β (1-40) in its fibrillar state was shown. This mechanism is GAG chain dependent. In addition, agrin accelerates A β fibril formation and contributes to larger fibrils than control samples. It can be hypothesized that agrin's GAG chains shield agrin and its associated proteins from proteolytic degradation, and may be responsible for the slow turnover of amyloid peptide aggregates (Cotman *et al.*, 2000).

Tissue culture studies have shown that agrin, when used as a substrate, inhibits neurite outgrowth (Bixby *et al.*, 2002; Campagna *et al.*, 1995; Halfter *et al.*, 1997). It is conceivable that the inhibitory activity of agrin contributes to the localization and termination of axons at particular sites of the muscle basement membrane by slowing the rate of axons outgrowth down. The neurite outgrowth inhibitory activity was localized to the N-terminal part of agrin, and it might be the heparan sulfate sidechains that provided the neurite outgrowth inhibitory function. This may explain the excessive growth of axons into the diaphragm in agrin knockout mice. The GAG chains may also prevent agrin from degradation, to ensure a long half-life of this protein at the NMJ.

4.4 Neurite outgrowth inhibition by agrin

The present study was aimed at determining the domains of agrin responsible for its neurite inhibitory effect. *In vitro* agrin is adhesive to neurons, can initiate synaptic vesicle clustering and can inhibit neurite outgrowth (Burg *et al.*, 1995; Campagna *et al.*, 1995; Campagna *et al.*, 1997; Chang *et al.*, 1997; Halfter *et al.*, 1997). It is conceivable that the inhibitory activity of agrin contributes to the localization and termination of axons at particular sites of the muscle basal lamina by slowing down the rate of axons outgrowth. This may explain the excessive growth of axons into the diaphragm in agrin knock-out mice. The neurite outgrowth inhibitory activity was localized to the N-terminal part of agrin, and it might be the GAG sidechains that provide this function.

Using various fragments of the N-terminal domains of agrin, DRGs were cultured on laminin-substrate adjacent to a stripe consisting of laminin-1 and the test-peptide. Neurites grew very well on the laminin-1 substrate and no inhibition induced by the test-stripe was found for protein fragments PF1, PF2, PF4, PF5 and PF8. For peptides PF3, PF7, and PF9 however, the test-stripe acted as a barrier for neurites. All three of these peptides possessed at least one of the two multiple GAG consensus sequences shown to be able to carry GAG sidechains (see chapters 3.3 and 4.3). To determine the influence of the GAG chains on this effect, the peptides PF7 and PF9 as well as the corresponding mutated peptides without the GAG chains (7Mc and 9Mc) were tested in the outgrowth assay. The mutated, unglycosylated peptides showed no neurite inhibition while the unmutated proteins functioned as barriers for neurites. This was true for both multiple GAG attachment sites of agrin. These results indicate that the GAG sidechains are the crucial factor for the neurite inhibition. These results are consistent with previous studies showing that the neurite outgrowth inhibition property of collagen IX is located in its CS sidechains (Halfter *et al.*, 1997). This study also investigated the influence of heparitinase treatment of agrin on its neurite outgrowth promoting activity. In contrast to the finding in the present study, Halfter *et al.* did not find a difference in the inhibitory properties of agrin after removal of the GAG sidechains. One explanation might be the incomplete removal of the GAG chains by the heparitinase.

4. Discussion

The type of carbohydrate attached to the core protein does not seem to be an important factor for the neurite outgrowth inhibitory effect. PF9 was shown to carry solely HS sidechains, while PF7 was shown to carry a mix of HS and CS sidechains (see chapter 3.3 and 4.3) and collagen IX carries only CS sidechains.

5. Literature

- Aricescu, A.R., McKinnell, I.W., Halfter, W. and Stoker, A.W. (2002) Heparan sulfate proteoglycans are ligands for receptor protein tyrosine phosphatase sigma. *Mol Cell Biol*, **22**, 1881-1892.
- Bause, E. (1983) Structural requirements of N-glycosylation of proteins. Studies with proline peptides as conformational probes. *Biochem J*, **209**, 331-336.
- Beck, K., Hunter, I. and Engel, J. (1990) Structure and function of laminin: anatomy of a multidomain glycoprotein. *Faseb J*, **4**, 148-160.
- Berger, E.A. and Shooter, E.M. (1977) Evidence for pro-beta-nerve growth factor, a biosynthetic precursor to beta-nerve growth factor. *Proc Natl Acad Sci U S A*, **74**, 3647-3651.
- Biroc, S.L., Payan, D.G. and Fisher, J.M. (1993) Isoforms of agrin are widely expressed in the developing rat and may function as protease inhibitors. *Brain Res Dev Brain Res*, **75**, 119-129.
- Bixby, J.L., Baerwald-De la Torre, K., Wang, C., Rathjen, F.G. and Ruegg, M.A. (2002) A neuronal inhibitory domain in the N-terminal half of agrin. *J Neurobiol*, **50**, 164-179.
- Bork, P. and Bairoch, A. (1995) poster. *Trends Biochem. Sci.*, **20**.
- Bourdon, M.A., Krusius, T., Campbell, S., Schwartz, N.B. and Ruoslahti, E. (1987) Identification and synthesis of a recognition signal for the attachment of glycosaminoglycans to proteins. *Proc Natl Acad Sci U S A*, **84**, 3194-3198.
- Brinkmann, T., Weilke, C. and Kleesiek, K. (1997) Recognition of acceptor proteins by UDP-D-xylose proteoglycan core protein beta-D-xylosyltransferase. *J Biol Chem*, **272**, 11171-11175.
- Burg, M.A., Halfter, W. and Cole, G.J. (1995) Analysis of proteoglycan expression in developing chicken brain: characterization of a heparan sulfate proteoglycan that interacts with the neural cell adhesion molecule. *J Neurosci Res*, **41**, 49-64.
- Burgess, R.W., Nguyen, Q.T., Son, Y.J., Lichtman, J.W. and Sanes, J.R. (1999) Alternatively spliced isoforms of nerve- and muscle-derived agrin: their roles at the neuromuscular junction. *Neuron*, **23**, 33-44.
- Burgess, R.W., Skarnes, W.C. and Sanes, J.R. (2000) Agrin isoforms with distinct amino termini: differential expression, localization, and function. *J Cell Biol*, **151**, 41-52.

- Burkin, D.J., Kim, J.E., Gu, M. and Kaufman, S.J. (2000) Laminin and alpha7beta1 integrin regulate agrin-induced clustering of acetylcholine receptors. *J Cell Sci*, **113** (Pt 16), 2877-2886.
- Bush, G.L., Tassin, A.M., Friden, H. and Meyer, D.I. (1991) Secretion in yeast. Purification and in vitro translocation of chemical amounts of prepro-alpha-factor. *J Biol Chem*, **266**, 13811-13814.
- Campagna, J.A., Ruegg, M.A. and Bixby, J.L. (1995) Agrin is a differentiation-inducing "stop signal" for motoneurons in vitro. *Neuron*, **15**, 1365-1374.
- Campagna, J.A., Ruegg, M.A. and Bixby, J.L. (1997) Evidence that agrin directly influences presynaptic differentiation at neuromuscular junctions in vitro. *Eur J Neurosci*, **9**, 2269-2283.
- Chang, D., Woo, J.S., Campanelli, J., Scheller, R.H. and Ignatius, M.J. (1997) Agrin inhibits neurite outgrowth but promotes attachment of embryonic motor and sensory neurons. *Dev Biol*, **181**, 21-35.
- Chen, R.L. and Lander, A.D. (2001) Mechanisms underlying preferential assembly of heparan sulfate on glypican-1. *J Biol Chem*, **276**, 7507-7517.
- Clontech. (2002) BD Talon Metal Affinity Resins User Manual.
- Cohen, C. and Parry, D.A. (1990) Alpha-helical coiled coils and bundles: how to design an alpha-helical protein. *Proteins*, **7**, 1-15.
- Cohen, I., Rimer, M., Lomo, T. and McMahan, U.J. (1997a) Agrin-induced postsynaptic-like apparatus in skeletal muscle fibers in vivo. *Mol Cell Neurosci*, **9**, 237-253.
- Cohen, N.A., Kaufmann, W.E., Worley, P.F. and Rupp, F. (1997b) Expression of agrin in the developing and adult rat brain. *Neuroscience*, **76**, 581-596.
- Colognato, H. and Yurchenco, P.D. (2000) Form and function: the laminin family of heterotrimers. *Dev Dyn*, **218**, 213-234.
- Cotman, S.L., Halfter, W. and Cole, G.J. (1999) Identification of extracellular matrix ligands for the heparan sulfate proteoglycan agrin. *Exp Cell Res*, **249**, 54-64.
- Cotman, S.L., Halfter, W. and Cole, G.J. (2000) Agrin binds to beta-amyloid (Abeta), accelerates abeta fibril formation, and is localized to Abeta deposits in Alzheimer's disease brain. *Mol Cell Neurosci*, **15**, 183-198.
- Denzer, A.J., Brandenberger, R., Gesemann, M., Chiquet, M. and Ruegg, M.A. (1997) Agrin binds to the nerve-muscle basal lamina via laminin. *J Cell Biol*, **137**, 671-683.

- Denzer, A.J., Gesemann, M., Schumacher, B. and Ruegg, M.A. (1995) An amino-terminal extension is required for the secretion of chick agrin and its binding to extracellular matrix. *J Cell Biol*, **131**, 1547-1560.
- Denzer, A.J., Schulthess, T., Fauser, C., Schumacher, B., Kammerer, R.A., Engel, J. and Ruegg, M.A. (1998) Electron microscopic structure of agrin and mapping of its binding site in laminin-1. *Embo J*, **17**, 335-343.
- Dolan, M., Horchar, T., Rigatti, B. and Hassell, J.R. (1997) Identification of sites in domain I of perlecan that regulate heparan sulfate synthesis. *J Biol Chem*, **272**, 4316-4322.
- Donahue, J.E., Berzin, T.M., Rafii, M.S., Glass, D.J., Yancopoulos, G.D., Fallon, J.R. and Stopa, E.G. (1999) Agrin in Alzheimer's disease: altered solubility and abnormal distribution within microvasculature and brain parenchyma. *Proc Natl Acad Sci U S A*, **96**, 6468-6472.
- Dong, S., Cole, G.J. and Halfter, W. (2002) Expression of collagen XVIII and localization of its glycosaminoglycan attachment sites. *J Biol Chem*.
- Ekblom, P. (1981) Formation of basement membranes in the embryonic kidney: an immunohistological study. *J Cell Biol*, **91**, 1-10.
- Ferns, M.J., Campanelli, J.T., Hoch, W., Scheller, R.H. and Hall, Z. (1993) The ability of agrin to cluster AChRs depends on alternative splicing and on cell surface proteoglycans. *Neuron*, **11**, 491-502.
- Gautam, M., Noakes, P.G., Moscoso, L., Rupp, F., Scheller, R.H., Merlie, J.P. and Sanes, J.R. (1996) Defective neuromuscular synaptogenesis in agrin-deficient mutant mice. *Cell*, **85**, 525-535.
- Gavel, Y. and von Heijne, G. (1990) Sequence differences between glycosylated and non-glycosylated Asn-X-Thr/Ser acceptor sites: implications for protein engineering. *Protein Eng*, **3**, 433-442.
- Gesemann, M., Cavalli, V., Denzer, A.J., Brancaccio, A., Schumacher, B. and Ruegg, M.A. (1996) Alternative splicing of agrin alters its binding to heparin, dystroglycan, and the putative agrin receptor. *Neuron*, **16**, 755-767.
- Gesemann, M., Denzer, A.J. and Ruegg, M.A. (1995) Acetylcholine receptor-aggregating activity of agrin isoforms and mapping of the active site. *J Cell Biol*, **128**, 625-636.
- Hagen, S.G., Michael, A.F. and Butkowski, R.J. (1993) Immunochemical and biochemical evidence for distinct basement membrane heparan sulfate proteoglycans. *J Biol Chem*, **268**, 7261-7269.
- Halfter, W. (1993) A heparan sulfate proteoglycan in developing avian axonal tracts. *J Neurosci*, **13**, 2863-2873.

- Halfter, W. (1998) Disruption of the retinal basal lamina during early embryonic development leads to a retraction of vitreal end feet, an increased number of ganglion cells, and aberrant axonal outgrowth. *J Comp Neurol*, **397**, 89-104.
- Halfter, W., Dong, S., Balasubramani, M. and Bier, M.E. (2001) Temporary disruption of the retinal basal lamina and its effect on retinal histogenesis. *Dev Biol*, **238**, 79-96.
- Halfter, W., Schurer, B., Yip, J., Yip, L., Tsen, G., Lee, J.A. and Cole, G.J. (1997) Distribution and substrate properties of agrin, a heparan sulfate proteoglycan of developing axonal pathways. *J Comp Neurol*, **383**, 1-17.
- Hopf, C. and Hoch, W. (1996) Agrin binding to alpha-dystroglycan. Domains of agrin necessary to induce acetylcholine receptor clustering are overlapping but not identical to the alpha-dystroglycan-binding region. *J Biol Chem*, **271**, 5231-5236.
- Imperiali, B. and Rickert, K.W. (1995) Conformational implications of asparagine-linked glycosylation. *Proc Natl Acad Sci U S A*, **92**, 97-101.
- Ishikawa, T., Terai, H. and Kitajima, T. (2001) Production of a biologically active epidermal growth factor fusion protein with high collagen affinity. *J Biochem (Tokyo)*, **129**, 627-633.
- Ji, R.R., Bose, C.M., Lesuisse, C., Qiu, D., Huang, J.C., Zhang, Q. and Rupp, F. (1998) Specific agrin isoforms induce cAMP response element binding protein phosphorylation in hippocampal neurons. *J Neurosci*, **18**, 9695-9702.
- Kammerer, R.A., Schulthess, T., Landwehr, R., Schumacher, B., Lustig, A., Yurchenco, P.D., Ruegg, M.A., Engel, J. and Denzer, A.J. (1999) Interaction of agrin with laminin requires a coiled-coil conformation of the agrin-binding site within the laminin gamma1 chain. *Embo J*, **18**, 6762-6770.
- Kawase, Y., Ohdate, Y., Shimojo, T., Taguchi, Y., Kimizuka, F. and Kato, I. (1992) Construction and characterization of a fusion protein with epidermal growth factor and the cell-binding domain of fibronectin. *FEBS Lett*, **298**, 126-128.
- Kjellen, L. and Lindahl, U. (1991) Proteoglycans: structures and interactions. *Annu Rev Biochem*, **60**, 443-475.
- Koch, M., Olson, P.F., Albus, A., Jin, W., Hunter, D.D., Brunken, W.J., Burgeson, R.E. and Champlaud, M.F. (1999) Characterization and expression of the laminin gamma3 chain: a novel, non-basement membrane-associated, laminin chain. *J Cell Biol*, **145**, 605-618.

- Kohfeldt, E., Maurer, P., Vannahme, C. and Timpl, R. (1997) Properties of the extracellular calcium binding module of the proteoglycan testican. *FEBS Lett*, **414**, 557-561.
- Kuhl, P.R. and Griffith-Cima, L.G. (1996) Tethered epidermal growth factor as a paradigm for growth factor- induced stimulation from the solid phase. *Nat Med*, **2**, 1022-1027.
- Lagenaur, C. and Lemmon, V. (1987) An L1-like molecule, the 8D9 antigen, is a potent substrate for neurite extension. *Proc Natl Acad Sci U S A*, **84**, 7753-7757.
- Ledent, P., Duez, C., Vanhove, M., Lejeune, A., Fonze, E., Charlier, P., Rhazi-Filali, F., Thamm, I., Guillaume, G., Samyn, B., Devreese, B., Van Beeumen, J., Lamotte-Brasseur, J. and Frere, J.M. (1997) Unexpected influence of a C-terminal-fused His-tag on the processing of an enzyme and on the kinetic and folding parameters. *FEBS Lett*, **413**, 194-196.
- Ma, E., Morgan, R. and Godfrey, E.W. (1994) Distribution of agrin mRNAs in the chick embryo nervous system. *J Neurosci*, **14**, 2943-2952.
- Mascarenhas, J.B., Ruegg, M.A., Winzen, U., Halfter, W., Engel, J. and Stetefeld, J. (2003) Mapping of the laminin-binding site of the N-terminal agrin domain (NtA). *Embo J*, **22**, 529-536.
- Maurer, P. and Engel, J. (1996) Structure of laminins and their chain assembly. *Harwood Academic Publishers*.
- Meier, T., Marangi, P.A., Moll, J., Hauser, D.M., Brenner, H.R. and Ruegg, M.A. (1998) A minigene of neural agrin encoding the laminin-binding and acetylcholine receptor-aggregating domains is sufficient to induce postsynaptic differentiation in muscle fibres. *Eur J Neurosci*, **10**, 3141-3152.
- Neumann, F.R., Bittcher, G., Annies, M., Schumacher, B., Kroger, S. and Ruegg, M.A. (2001) An alternative amino-terminus expressed in the central nervous system converts agrin to a type II transmembrane protein. *Mol Cell Neurosci*, **17**, 208-225.
- Nitkin, R.M., Smith, M.A., Magill, C., Fallon, J.R., Yao, Y.M., Wallace, B.G. and McMahan, U.J. (1987) Identification of agrin, a synaptic organizing protein from Torpedo electric organ. *J Cell Biol*, **105**, 2471-2478.
- O'Connor, L.T., Lauterborn, J.C., Gall, C.M. and Smith, M.A. (1994) Localization and alternative splicing of agrin mRNA in adult rat brain: transcripts encoding isoforms that aggregate acetylcholine receptors are not restricted to cholinergic regions. *J Neurosci*, **14**, 1141-1152.

- Patthy, L. and Nikolics, K. (1993) Functions of agrin and agrin-related proteins. *Trends Neurosci*, **16**, 76-81.
- Reist, N.E., Werle, M.J. and McMahan, U.J. (1992) Agrin released by motor neurons induces the aggregation of acetylcholine receptors at neuromuscular junctions. *Neuron*, **8**, 865-868.
- Roden, L., Koerner, T., Olson, C. and Schwartz, N.B. (1985) Mechanisms of chain initiation in the biosynthesis of connective tissue polysaccharides. *Fed Proc*, **44**, 373-380.
- Ruegg, M.A. and Bixby, J.L. (1998) Agrin orchestrates synaptic differentiation at the vertebrate neuromuscular junction. *Trends Neurosci*, **21**, 22-27.
- Ruegg, M.A., Tsim, K.W., Horton, S.E., Kroger, S., Escher, G., Gensch, E.M. and McMahan, U.J. (1992) The agrin gene codes for a family of basal lamina proteins that differ in function and distribution. *Neuron*, **8**, 691-699.
- Sasaki, M. and Yamada, Y. (1987) The laminin B2 chain has a multidomain structure homologous to the B1 chain. *J Biol Chem*, **262**, 17111-17117.
- Stetefeld, J., Jenny, M., Schulthess, T., Landwehr, R., Schumacher, B., Frank, S., Ruegg, M.A., Engel, J. and Kammerer, R.A. (2001) The laminin-binding domain of agrin is structurally related to N-TIMP-1. *Nat Struct Biol*, **8**, 705-709.
- Sugiyama, J.E., Glass, D.J., Yancopoulos, G.D. and Hall, Z.W. (1997) Laminin-induced acetylcholine receptor clustering: an alternative pathway. *J Cell Biol*, **139**, 181-191.
- Timpl, R. and Brown, J.C. (1994) The laminins. *Matrix Biol*, **14**, 275-281.
- Timpl, R. and Brown, J.C. (1996) Supramolecular assembly of basement membranes. *Bioessays*, **18**, 123-132.
- Tsen, G., Halfter, W., Kroger, S. and Cole, G.J. (1995) Agrin is a heparan sulfate proteoglycan. *J Biol Chem*, **270**, 3392-3399.
- Ullrich, A., Gray, A., Berman, C. and Dull, T.J. (1983) Human beta-nerve growth factor gene sequence highly homologous to that of mouse. *Nature*, **303**, 821-825.
- Wiberg, C., Hedbom, E., Khairullina, A., Lamande, S.R., Oldberg, A., Timpl, R., Morgelin, M. and Heinegard, D. (2001) Biglycan and decorin bind close to the n-terminal region of the collagen VI triple helix. *J Biol Chem*, **276**, 18947-18952.
- Zhang, L., David, G. and Esko, J.D. (1995) Repetitive Ser-Gly sequences enhance heparan sulfate assembly in proteoglycans. *J Biol Chem*, **270**, 27127-27135.

Zhang, L. and Esko, J.D. (1994) Amino acid determinants that drive heparan sulfate assembly in a proteoglycan. *J Biol Chem*, **269**, 19295-19299.

6. Zusammenfassung

Agrin ist ein ca. 200 kDa großes Protein und Hauptbestandteil fast aller Basalmembranen. Es besteht aus verschiedenen Domänen und trägt einen hohen Anteil an Kohlenhydratseitenketten und wurde bereits als Heparansulfat-Proteoglykan (HSPG) identifiziert. Agrin ist essentiell an der Entstehung neuromuskulärer Verbindungen beteiligt, wie aus dem Phänotyp der knock-out Mäuse zu erkennen ist.

Während die C-terminale Hälfte des Moleküls bereits detailliert untersucht wurde, ist über die N-terminale Hälfte des Moleküls wenig bekannt. Es ist bekannt, dass Agrin mit der N-terminalen Domäne (NtA) an das Basalmembranprotein Laminin-1 bindet. Darüberhinaus wurde gezeigt, dass in der N-terminalen Hälfte des Proteins die Bindungsstellen für die HS-Seitenketten lokalisiert sind

In der vorliegenden Arbeit wurde die NtA-Domäne exprimiert und ihre Wechselwirkung mit Laminin-1 in ELISA-Assays untersucht. Da die Wechselwirkung zwischen Agrin und Laminin vermutlich ionischer Natur ist, wurden positiv geladene Aminosäuren in der NtA mittels site-directed mutagenesis in neutrale Aminosäuren umgewandelt. Hierbei zeigte sich, dass 2 Aminosäuren einen besonders grossen Einfluss auf die Lamininbindung haben. In Zusammenarbeit mit dem Biozentrum in Basel wurden die Aminosäuren, die an der Interaktion zwischen Laminin und Agrin beteiligt sind genau bestimmt. Es konnte gezeigt werden, dass an der Bindung des Laminins nicht nur geladene Aminosäuren sondern auch hydrophobe Aminosäuren beteiligt sind.

Die Fusion der NtA-Domäne mit dem Nerve growth factor (NGF) ergibt ein Fusionsprotein, das mit hoher Affinität an Laminin bindet. Dies zeigt, dass die NtA-Domäne als target-Modul in Fusionsproteinen verwendet werden kann.

Der Hauptteil der vorliegenden Arbeit befasste sich mit der Lokalisierung der HS-Seitenketten innerhalb des Proteins. Die Expression verschiedener Agrin-Fragmente, kombiniert mit site-directed mutagenesis Experimenten zeigte, dass von über 20 SG-Konsensussequenzen nur 7 in der Lage sind HS-Ketten zu tragen. Diese 7 Konsensussequenzen sind in 2 Clustern konzentriert. Ein Vergleich mit anderen Proteoglykanen zeigte, dass eine Glykosylierungsstelle und der Typ der Seitenkette mit

relativ hoher Wahrscheinlichkeit, aber nicht absoluter Sicherheit vorhergesagt werden kann.

Desweiteren konnte mit Hilfe von *neurite outgrowth assays* gezeigt werden, dass diese Glycosaminoglykan (GAG) Seitenketten für den inhibitorischen Effekt von Agrin auf Neuriten verantwortlich sind.

7. Abstract

Agrin, a major component of all basal membranes, is a key organizer of acetylcholine receptor (AChR) clustering at the vertebrate neuromuscular junction (NMJ). Agrin deficient mice are paralyzed and die at birth due to malfunctioning NMJs in the diaphragm. Agrin is highly glycosylated and it has been identified as a heparan sulfate proteoglycan (HSPG).

While extensive studies have been conducted on the C-terminal half of the molecule, rather little is known about the N-terminal half of the protein. Previous studies have shown that the N-terminal domain (NtA) is required for the laminin-binding property of agrin, but the mechanism underlying this high affinity interaction remains elusive.

In the present study, the NtA-domain of agrin was expressed and its interaction with laminin was examined by solid phase binding assays. Because the binding mechanism is thought to involve ionic interactions between positively charged amino acids of the NtA and negatively charged amino acids of the laminin coiled coil domain, site directed mutagenesis experiments were conducted. In cooperation with the biocenter in Basel, this study was able to show that the interaction between laminin-1 and agrin is solely conducted by the NtA-domain. It was revealed that charged as well as hydrophobic amino acids are involved in the mechanism.

Utilizing the laminin-binding property of this domain, this study attempted to create a fusion protein of NGF and the NtA-domain of agrin. The results showed that the NtA-domain can in fact be used to target NGF to specific locations, e.g. the basal lamina.

The main focus of this work was on localizing the attachment sites for the heparan sulfate sidechains of agrin. Recombinant expression of agrin fragments and site-directed mutagenesis experiments showed that of all 20 SG-consensus sequences within the agrin core-proteins, only 7 are capable of carrying glycosaminoglycan (GAG) side chains. These 7 SGs are concentrated within 2 major clusters. A comparison with other proteoglycans revealed that a combination of acidic amino acids preceding a cluster of SG-dipeptides promotes the priming of HS side chains in a core protein. However

glycosylation cannot be predicted with absolute certainty based on the current knowledge of GAG priming.

Neurite outgrowth assays with various fragments and mutants of agrin revealed that the GAG sidechains are responsible for the neurite outgrowth inhibition of agrin.

8. Acknowledgments

I would like to thank:

Prof. Dr. Waffenschmidt for her role as the *Doctorvater* of my thesis and for all her work involving this position.

Prof. Willi Halfter for giving me the opportunity to work in his lab, his constant support and advice and for being a great person.

Mark Parrish for giving me valuable feedback on the manuscript.

I also want to thank Addie for her constant support and reading the manuscript over and over again.

Most of all I want to thank my parents and my sister for supporting me in every way possible. It would not have been possible without you.

Erklärung

Ich versichere, daß ich die von mir vorgelegte Dissertation selbständig angefertigt, die benutzten Quellen und Hilfsmittel vollständig angegeben und die Stellen der Arbeit - einschließlich Tabellen, Karten und Abbildungen -, die anderen Werken im Wortlaut oder dem Sinn nach entnommen sind, in jedem Einzelfall als Entlehnung kenntlich gemacht habe; daß diese Dissertation noch keiner anderen Fakultät oder Universität zur Prüfung vorgelegen hat; daß sie - abgesehen von unten angegebenen Teilpublikationen - noch nicht veröffentlicht worden ist sowie, daß ich eine solche Veröffentlichung vor Abschluß des Promotionsverfahrens nicht vornehmen werde. Die Bestimmungen dieser Promotionsordnung sind mir bekannt. Die von mir vorgelegte Dissertation ist von Prof. Dr. Sabine Waffenschmidt betreut worden.

Pittsburgh, den 25.02.2003

Uwe Winzen

Teilpublikationen:

Mascarenhas, J.B., Ruegg, M.A., **Winzen, U.**, Halfter, W., Engel, J. and Stetefeld, J. (2003) Mapping of the laminin-binding site of the N-terminal agrin domain (NtA). *Embo J*, **22**, 529-536.

Winzen, U., Cole, G.J., and Halfter, W. (2003) Localization of the glycosaminoglycan attachment sites reveals that agrin is a chimeric heparan sulfate/chondroitin sulfate proteoglycan, *JBC*, **in review**

Uwe Winzen
Kolmarerstr.13
D-50769 Köln

Lebenslauf

Name	Uwe Winzen
Geburtsdatum	11. Oktober 1973
Geburtsort	Köln
Familienstand	ledig
Schulbesuch	1980 – 1984 GSG Spoerkelhof, Merkenich, Köln
	1984 – 1993 Blüchergymnasium, Nippes, Köln
Schulabschluss	Mai 1993 Allgemeine Hochschulreife
Wehrdienst	07/93 – 06/94 Stabskompanie III.Korps, Koblenz
Studium	10/94 – 12/99 Studium der Chemie, Universität zu Köln Abschluss: Diplom-Chemiker Wahlfach: Physiologische Chemie (chemische Richtung) Diplomarbeit: Diplomarbeit am Institut für Biochemie II der medizinischen Fakultät der Universität zu Köln. Thema: „Synthese rekombinanter Protein-fragmente der Proteoglykane Testican -2 und -3 zur Herstellung spezifischer Antiseren und deren Charakterisierung“ Supervisor: Prof. Dr. Mats Paulsson
Doktorarbeit	seit 01/00 Dissertation am Institut für Biochemie, Universität zu Köln Durchführung der Experimente an der Universität zu Pittsburgh, Pennsylvania, USA Thema: „Functional analysis of the N-terminal domains of agrin by recombinant eucaryotic expression“ Supervisor: Prof. Dr. Sabine Waffenschmidt